Integration of Genome-Scale Metabolic Model with Biorefinery Process Model Reveals Market-Competitive Carbon-Negative Sustainable Aviation Fuel Utilizing Microbial Cell Mass Lipids and Biogenic CO_2

Nawa Raj Baral,[a,b,*] Deepanwita Banerjee,[a,b] Aindrila Mukhopadhyay,[a,b] Blake A. Simmons,[a,b] Steven W. Singer,[a,b] and Corinne D. Scown [a,b,c,d]

** Corresponding author: nrbaral@lbl.gov*

DOI: 10.15376/biores.19.3.4056-4086

GRAPHICAL ABSTRACT

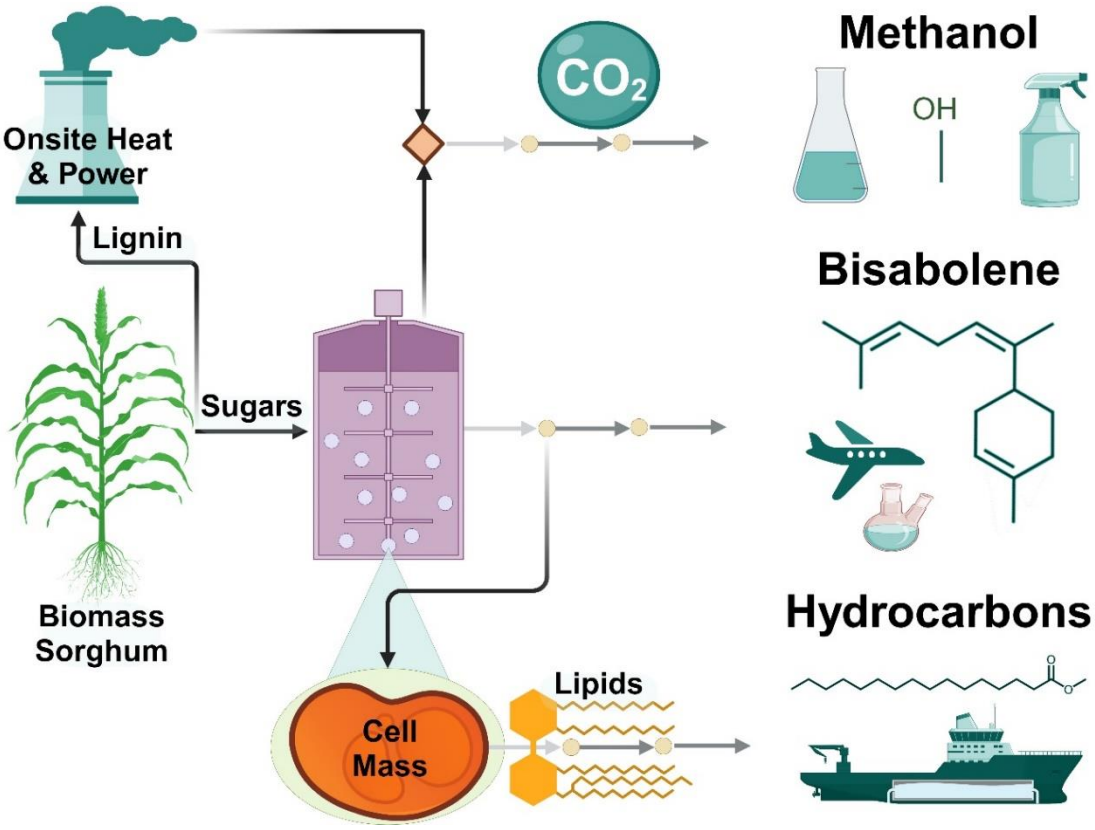

Integration of Genome-Scale Metabolic Model with Biorefinery Process Model Reveals Market-Competitive Carbon-Negative Sustainable Aviation Fuel Utilizing Microbial Cell Mass Lipids and Biogenic CO_2

Nawa Raj Baral,[a,b,*] Deepanwita Banerjee,[a,b] Aindrila Mukhopadhyay,[a,b] Blake A. Simmons,[a,b] Steven W. Singer,[a,b] and Corinne D. Scown [a,b,c,d]

Producing scalable, economically viable, low-carbon biofuels or biochemicals hinges on more efficient bioconversion processes. While microbial conversion can offer robust solutions, the native microbial growth process often redirects a large fraction of carbon to CO_2 and cell mass. By integrating genome-scale metabolic models with techno-economic and life cycle assessment models, this study analyzes the effects of converting cell mass lipids to hydrocarbon fuels, and CO_2 to methanol on the facility's costs and life-cycle carbon footprint. Results show that upgrading microbial lipids or both microbial lipids and CO_2 using renewable hydrogen produces carbon-negative bisabolene. Additionally, on-site electrolytic hydrogen production offers a supply of pure oxygen to use in place of air for bioconversion and fuel combustion in the boiler. To reach cost parity with conventional jet fuel, renewable hydrogen needs to be produced at less than $2.2 to $3.1/kg, with a bisabolene yield of 80% of the theoretical yield, along with cell mass and CO_2 yields of 22 wt% and 54 wt%, respectively. The economic combination of cell mass, CO_2, and bisabolene yields demonstrated in this study provides practical insights for prioritizing research, selecting suitable hosts, and determining necessary engineered production levels.

DOI: 10.15376/biores.19.3.4056-4086

Keywords: Biomass sorghum; Microbial lipids; Carbon capture and utilization; Renewable hydrogen; Hydrocarbon fuel; Sustainable aviation fuel; eFuels

*Contact information: a: Joint BioEnergy Institute, Lawrence Berkeley National Laboratory, Berkeley, California 94720, United States; b: Biological Systems and Engineering Division, Lawrence Berkeley National Laboratory, Berkeley, California 94720, United States; c: Energy Analysis and Environmental Impacts Division, Lawrence Berkeley National Laboratory, Berkeley, California 94720, United States; d: Energy & Biosciences Institute, University of California, Berkeley, California 94720, United States; * Corresponding author: nrbaral@lbl.gov*

INTRODUCTION

Genome-scale metabolic modeling, combined with experimental studies, is gaining popularity for enhancing the titer, rate, and yield of biofuels or biochemicals (Banerjee *et al.* 2020). It is essential to integrate genome-scale metabolic models, experimental findings, and biorefinery process models using techno-economic analysis and lifecycle assessment tools for the development of scalable, economically viable, carbon-neutral, or carbon-negative biomass-derived renewable fuels, chemicals, and materials. This study aims to bridge this critical research gap by focusing on a field-to-biofuel production model, particularly emphasizing the determination of the economic viability and carbon footprint

of high-energy-density biofuels suitable for challenging-to-electrify sectors such as aviation and marine applications.

Breakthroughs in identifying high-energy-density renewable jet fuel precursors, such as monoterpenes (C10) and sesquiterpenes (C15), have been achieved at the bench scale (Liu *et al.* 2018; Li *et al.* 2023). These biofuel molecules, including: limonene, 1,8-cineole, linalool, farnesene, bisabolene, and epi-isozizaene, can be converted into saturated forms (alkanes) through hydrogenation or oligomerization/hydrogenation processes ensuring optimal performance when blended into jet fuel (Li *et al.* 2023; Baral *et al.* 2019). In addition to terpenoids, isoprenol, a platform chemical (Keller *et al.* 2023), can be catalytically upgraded into 1,4-dimethylcyclooctane (DMCO), which has a volumetric heat of combustion about 9.2% higher than petroleum Jet-A (Rosenkoetter *et al.* 2019), potentially leading to substantial fuel savings or extended aircraft range upon commercial implementation (Baral *et al.* 2019).

Assessing the progress towards achieving high energy-density biofuel molecules through the biochemical conversion process reveals a need for substantial improvements, particularly in the microbial bioconversion stage (Baral *et al.* 2019; Aggarwal *et al.* 2023). The challenge lies in engineering host microbes to efficiently convert both hexose (mainly glucose) and pentose (mainly xylose) sugars derived from biomass, while maximizing the production rate, quantity (titer), and efficiency (yield) of biofuels or biochemicals. In most early stages of the bioconversion process, a majority of carbon sources result in cell mass and CO_2, yielding only a small fraction of the main target product. Here, we provide a critical assessment of the impact of upgrading cell mass lipids into hydrocarbon fuel, and CO_2 into methanol in a typical biorefinery setup on economic feasibility and climate impacts. This analysis emphasizes the importance of early-stage system-level evaluations to critically assess potential bioconversion process optimization opportunities, assisting in prioritizing future research and development efforts.

The advancements in synthetic biology and metabolic engineering show significant promise in improving the titer, rate, and yield of target molecules. This potential extends to achieving pathway-dependent theoretical yields using various microbial hosts: *Escherichia coli*, *Pseudomonas putida*, *Rhodosporidium toruloides*, and *S. cerevisiae* (Kirby *et al.* 2021; Liu *et al.* 2021; Wang *et al.* 2022a; Wang *et al.* 2022b; Huang *et al.* 2023). The majority of reported titers, rates, and yields of terpenes from bench-scale studies (Table A1) are below 5 g/L, 0.15 g/L/h, and 35% of the theoretical yield, primarily utilizing glucose as the sole carbon source. Isoprenol exhibits a range of titer, rate, and yield, spanning from 8.5 to 12.4 g/L, 0.1 to 0.15 g/L/h, and 34 to 44 % of the maximum theoretical yield (Wang *et al.* 2022a; Kim and Lee 2023; Kang *et al.* 2019). However, even if the theoretical yield is achieved, approximately 60 to 70% of starting carbon material is not converted to the desired molecule. While various bench-scale studies (Table A1) reported nearly 100% utilization of carbon sources (Perez-Pimienta *et al.* 2019; Walls *et al.* 2023), it is apparent that the initial carbon that does not go to the desired product will lead to CO_2 emissions and the formation of cell mass. Typically, CO_2 emission is not measured during microbial strain development at laboratory scale. The lack of comprehensive experimental mass balance data poses challenges in precisely attributing initial carbon materials to cell mass, CO_2, and other metabolites. Nevertheless, both CO_2 and cell mass offer opportunities to reconfigure conventional biorefineries, wherein CO_2 is released into the atmosphere and cell mass is burned onsite for heat and power, considering their high-value potential.

When considering the conversion of CO_2 and cell mass into high-value products, some crucial questions arise: is it economically advantageous and does it effectively reduce

overall GHG emissions of the primary product? If so, determining a combination of CO_2, cell mass, and biofuel yield for processes that produce economically viable low carbon biofuel becomes pivotal. This question persists, particularly considering the low theoretical yield of high energy-density biofuel molecules and the challenges associated with achieving yields close to the theoretical limit. This study addresses these questions by developing a system-level process model that considers biomass sorghum as a representative biomass, *R. toruloides* as a representative host microbe, and bisabolene as a representative biofuel molecule.

The selection of *R. toruloides*—an oleaginous, carotenogenic basidiomycete yeast—is primarily due to its ability to simultaneously metabolize diverse carbon sources, including pentose and hexose sugars, and aromatics derived from lignocellulosic biomass (Kirby *et al.* 2021; Walls *et al.* 2023; Yaegashi *et al.* 2017). It can accumulate a high concentration of lipids, making it a promising host for the production of lipid-based bioproducts, and it has a much greater tolerance for inhibitory byproducts of lignin depolymerization such as vanillin and furfural (Walls *et al.* 2023; Yaegashi *et al.* 2017) as well as tolerance for lignin pretreatment chemicals such as ionic liquids (Sundstrom *et al.* 2018). The advances in genetic toolsets (Nora *et al.* 2019; Otoupal *et al.* 2019), well-curated genome-scale metabolic models (Dinh *et al.* 2019; Kim *et al.* 2021), and the availability of omics data in *R. toruloides* (Zhu *et al.* 2012) further promise great potential for this organism as one of the popular microbial chassis for advanced bioconversions.

Bisabolene is selected as a representative biofuel molecule produced in *R. toruloides* as a single product, facilitating its recovery with high purity. It can be hydrogenated to bisabolane, which has excellent combustion properties similar to petroleum-derived fuels, holding great promise as a "drop-in" replacement for diesel and jet fuels (Peralta-Yahya *et al.* 2012; Butcher *et al.* 2018; Staples *et al.* 2019), as the use of a single fuel molecule without modifying existing engines is unlikely. While its testing in commercial flights is still needed, the implications and impacts of its use phase are out of the scope of this study. The goal here is to integrate techno-economic analysis (TEA), life cycle assessment (LCA), and genome-scale metabolic engineering models. This study also aims to identify process bottlenecks, optimization prospects, and crucial performance thresholds. Such insights can guide future research and, ultimately, provide actionable strategies for selecting suitable hosts and determining the necessary level of engineering.

EXPERIMENTAL

Modeling Overview

This study has developed a field-to-biorefinery process model designed to utilize a nameplate capacity of 2000 bone-dry metric tons (bdt) of biomass sorghum per day. Figure 1 presents an overview of the primary production stages. The baseline biorefinery encompasses biomass production and supply, biomass deconstruction, bioconversion, recovery and separation, wastewater treatment, and onsite energy and utility stages. This basic biorefinery undergoes enhancement by integrating CO_2-to-methanol and cell mass lipids conversion into primarily diesel range hydrocarbon fuels. In the baseline biorefinery setup, CO_2 is emitted into the atmosphere while the cell mass is directed to the onsite heat and power generation unit. Previous studies (Humbird *et al.* 2011; Baral *et al.* 2019) offer detailed assessments of conventional lignocellulosic biorefineries. Subsequent sections

provide concise descriptions of all production stages considered in this study and delineate the modifications introduced herein.

Biomass production and supply

The production and supply of biomass encompass several components, including: biomass sorghum cultivation, in-field operations, transportation, and storage. Biomass production relies on a rain-fed system, resulting in a biomass yield of 22.4 bdt/ha (10 tons per acre) (Huntington *et al.* 2020). In-field operations consist of windrowing, conditioning (to break hard stems of biomass), field drying, baling, and stacking biomass bales at the field edge. These biomass bales are then transported to the biorefinery using 5-axle tractor semi-trailers and stored adjacent to the biorefinery under tarps. It is assumed that the delivered biomass has a moisture content of 20% (Baral *et al.* 2020). Detailed descriptions of modeling methodologies and data inputs concerning biomass production and the supply chain have been documented in the authors' previous work (Baral *et al.* 2020). Table 1 summarizes the resulting costs and GHG emissions of the delivered biomass feedstock at the biorefinery gate.

Biomass preprocessing

The delivered biomass bales are transported *via* a conveyor belt to the shredder and subsequently to the hammer mill to break them down into the desired particle size of 6.35 mm (Aden *et al.* 2002). The milled biomass is temporarily stored before being transported to the biomass deconstruction unit. Assumptions and data sources for biomass preprocessing are consistent with the authors' prior work (Baral *et al.* 2020).

Biomass deconstruction

The biomass deconstruction process involves several stages: pretreatment, neutralization, enzymatic hydrolysis, and ionic liquid (IL) recovery. This study considered a biocompatible ionic liquid, cholinium lysinate ([Ch][Lys]), which is very effective for biomass pretreatment at a low concentration, such as 2.5 to 5% by mass of the whole hydrolysate, and releases clean sugar without microbial inhibitors such as HMF and furfural (Rodriguez *et al.* 2019), due to the low severity pretreatment conditions considered in this study. During the biomass deconstruction process, initially, the biomass is combined with IL and water to achieve an IL loading of 5 wt% and solid loading of 30 wt% (Magurudeniya *et al.* 2021). This prepared mixture is then directed into the pretreatment reactor, where it undergoes pretreatment at 140 °C for 1 h (Sundstrom *et al.* 2018; Magurudeniya *et al.* 2021).

Following biomass pretreatment, the pretreated slurry is transported to the neutralization unit. Sulfuric acid (93%) is incorporated at a loading rate of 0.1 kg of sulfuric acid per kg of ionic liquid (IL) into the pretreated slurry to adjust the pH (Magurudeniya *et al.* 2021). This results in an overall sulfuric acid concentration in the whole slurry of 0.3% by mass. Following this, the entire mixture is subsequently transferred to the enzymatic hydrolysis reactor.

Within the enzymatic hydrolysis reactor, a blend of cellulase enzymes, at a concentration of 10 mg of protein/g of glucan, is introduced (Magurudeniya *et al.* 2021). Water is added to achieve an initial solid loading of 25 wt% (Magurudeniya *et al.* 2021). After hydrolysis, solids and liquids are separated using a vacuum belt filter, followed by ultrafiltration. The solid fraction is directed to the boiler for the generation of onsite heat and power, while the liquid fraction is transferred to the IL recovery unit.

In the IL recovery unit, 99% of the IL is recovered through a pervaporation system (Sun *et al*. 2017) and recycled back to the pretreatment reactor. The resulting sugar solution, mainly glucose and xylose, is directed to the bioconversion unit, while any unrecovered liquid is routed to the wastewater treatment unit. Previous studies extensively discuss the modeling assumptions related to the biomass deconstruction process, and the primary data inputs are summarized in Table 1.

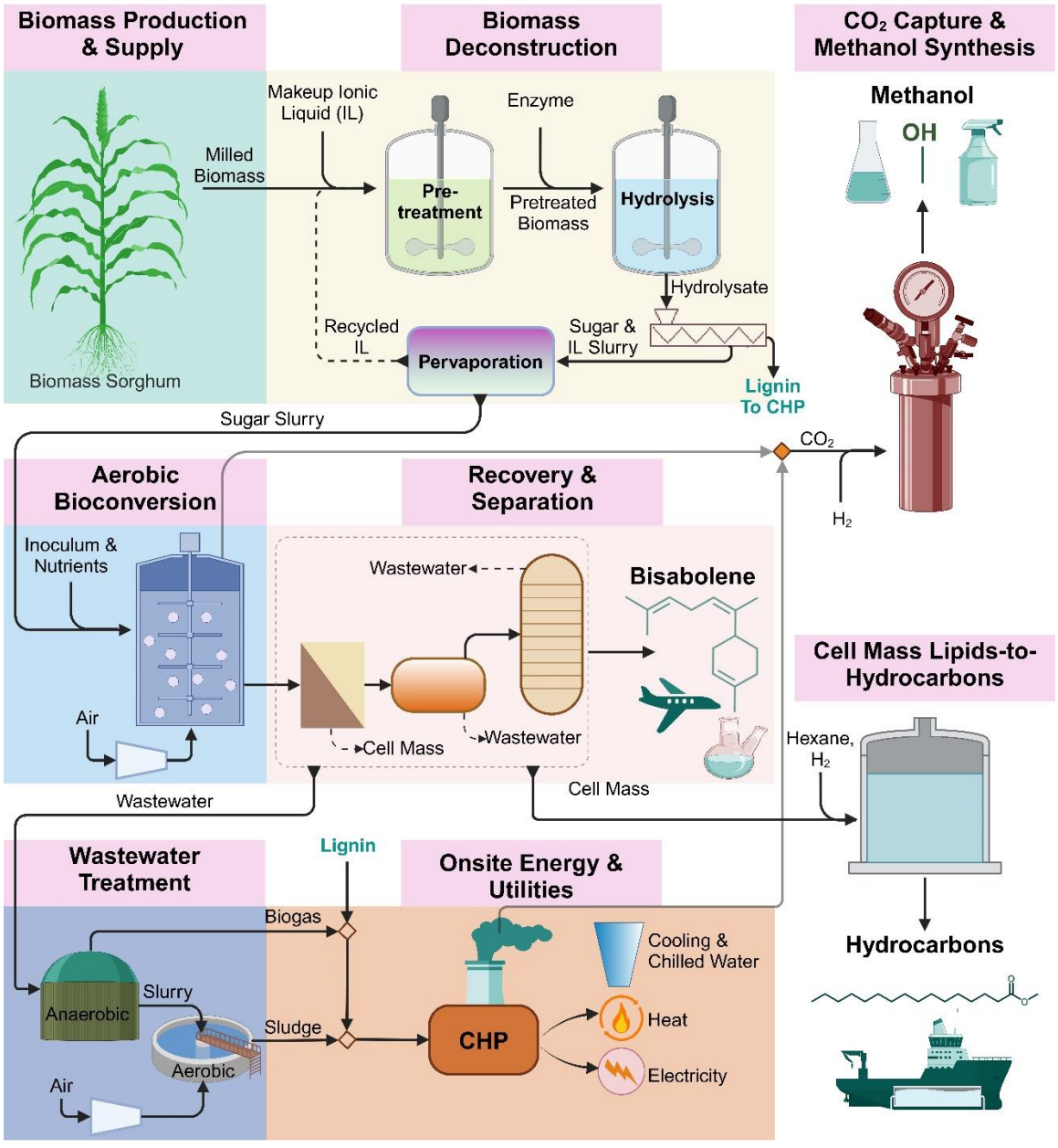

Fig. 1. Overview of biorefinery process model developed in this study

Bioconversion

Nitrogen sources, such as corn steep liquor, diammonium phosphate, and ammonia, along with inoculum (*R. toruloides*, fully cultivated in a seed reactor), are combined with a sugar solution and fed into the primary bioconversion reactor. An air compressor supplies air to both the seed and main reactors. *R. toruloides* metabolizes glucose and xylose, predominantly found in the sugar solution, to produce bisabolene. To ensure uniform dissolved oxygen concentration, a 1000 m^3 bubble column bioreactor is employed in this study (Davis *et al.* 2018). Following bioconversion, the entire slurry is directed to the recovery and separation unit. In the baseline scenario, CO_2 and other gases discharged from the bioreactor are released into the atmosphere. Conversely, in the CO_2 utilization scenario, these gases are channeled to the CO_2-to-methanol conversion unit for CO_2 capture and utilization. Table 1 provides an overview of the principal modeling inputs, which remain consistent with previous studies.

Recovery and separation

After bioconversion, the entire slurry undergoes decantation and microfiltration processes to eliminate the cell mass. Bisabolene extraction from the liquid fraction involves decantation followed by distillation, assuming an overall bisabolene recovery rate of 98% (Baral *et al.* 2019). The recovered bisabolene is stored onsite. In the baseline scenario, the recovered cell mass is directed to the boiler, while any wastewater and residual materials are conveyed to the wastewater treatment unit. However, in the scenario involving cell mass utilization, the recovered cell mass is diverted to the cell mass lipids-to-hydrocarbon fuels conversion unit for further processing. Table 1 summarizes major data inputs for the recovery and separation units, aligned with prior studies.

Wastewater treatment

The wastewater undergoes treatment through successive anaerobic and aerobic processes. Within an anaerobic digester, 86% of the organic matter in the wastewater is converted into biogas, while 5% is transformed into cell mass (Humbird *et al.* 2011). Both the generated biogas and recovered digester sludge (cell mass) are directed to the boiler for the production of heat and power. The treated water is stored on-site and utilized as process water. All modeling assumptions for the wastewater treatment process align with previous studies (Aden *et al.* 2002; Humbird *et al.* 2011), and significant data inputs are outlined in Table 1.

Onsite energy and utilities

The bisabolene biorefinery designed in this study utilizes unused solid biomass residues (primarily lignin), cell mass, and biogas. If these sources are insufficient to meet the facility's electricity needs, additional electricity is obtained from the grid (using the U.S. electricity mix). In addition to process steam and electricity, this unit supplies makeup process water, cooling water, chilled water, and chemicals for cleaning and sterilization. The modeling assumptions in this section align with those of previous studies (Aden *et al.* 2002; Humbird *et al.* 2011). In the baseline scenario, the flue gas is discharged into the atmosphere, while in the CO_2 utilization scenario, the flue gas is directed towards the CO_2-to-methanol conversion unit. Table 1 outlines the major data inputs.

Conversion of CO_2 into methanol

The CO_2-to-methanol conversion process consists of two stages: initially capturing CO_2 from a blend of bioreactor off-gas and flue gas, followed by the methanol synthesis stage. This study considers established amine scrubbing methods to capture CO_2 and then catalytic hydrogenation of CO_2 to methanol. While methanol finds diverse applications, such as a fuel additive and a precursor for polymers (Harris *et al.* 2021), the authors acknowledge the potential for developing higher value-added fuels or chemicals from CO_2 (Do *et al.* 2022), currently under development at a larger scale (Liew *et al.* 2022).

In this study, the bioreactor off-gas and the flue gas from the boiler are combined and directed to the absorption unit, where a 30 wt% monoethanolamine (MEA) solution is introduced to achieve a targeted molar concentration of 0.21 mol CO_2 per mol of MEA (Ramezan *et al.* 2007; Bravo *et al.* 2021; Wang *et al.* 2023). The resulting CO_2-MEA rich mixture proceeds to the stripping stage, where MEA is regenerated and recycled back to the absorption unit. The gases and water vapor exiting the stripper are condensed to eliminate water, resulting in 99% pure CO_2 (Wang *et al.* 2013). The assumed overall CO_2 capture efficiency in this process is 90% (Wang *et al.* 2013).

Following the amine scrubbing process, the CO_2-rich gas is initially directed to the H_2S removal unit, employing a ZnO catalyst to reduce sulfur to undetectable levels. This sulfur removal is crucial to safeguard the methanol synthesis catalyst from sulfur-induced deactivation. For methanol synthesis, a copper/zinc oxide/alumina catalyst is utilized, operating at a gas hourly space velocity of 8000 /h (Tan *et al.* 2015). Hydrogen is combined with nearly pure CO_2 gas at a mass ratio of 0.137 %, compressed to a pressure of 51 bar, and then supplied to the methanol synthesis reactor (Tan *et al.* 2015). The reactor functions isothermally at 250 °C (Tan *et al.* 2015), facilitating the primary conversion of CO_2 into CO, subsequently transforming into methanol. In a single pass, 46 % of the CO is converted into methanol.

Vapor-phase methanol derived from the methanol synthesis reactor undergoes condensation and separation from the unreacted gases. Roughly 95 wt% of the unconverted gases are recycled back into the methanol synthesis reactor, while the remainder is directed to the boiler (Tan *et al.* 2015). The overall methanol recovery is assumed to be 98%. The recovered methanol undergoes further purification via distillation to eliminate water. Previous studies provide detailed descriptions of the amine scrubbing and methanol synthesis processes, which remain consistent in this study and are summarized in Table 1.

Conversion of cell mass into hydrocarbon fuels

Microbial cell mass (*R. toruloides*) contains about 60 to 68 wt% lipid (Li *et al.* 2007; Yaegashi *et al.* 2017). In a prior study (Yaegashi *et al.* 2017), similar levels of lipids were reported in both engineered and wild-type *R. toruloides* strains, although the actual lipid content could vary once the microbes are fully engineered. From a modeling standpoint, it is expected that the future optimal *R. toruloides* strain will contain a similar level of lipids as the wild type, but the total microbial mass will be reduced, as supported by our metabolic model. This microbial lipid is a potential precursor for biofuels and bioproducts, including industrial products and nutrient-rich foods. For the purposes of this study, we study the impacts of microbial lipids utilization on the production cost and carbon footprint of bisabolene by converting it into hydrocarbon fuels.

A typical product composition of the reactor includes 78.5 wt% diesel-range and 1.5 wt% jet fuel-range hydrocarbon fuels, 5.6 wt% propane, 12.1 wt% CO_2, 0.6 wt% CO, and 1.7 wt% H_2O (Jones *et al.* 2014).

The process model for converting cell mass lipids into hydrocarbon fuels, along with its underlying assumptions, is consistent with a model previously developed by NREL for the conversion of algal-lipid into hydrocarbon fuels (Jones *et al.* 2014). In this process, the cell mass undergoes microbial lipid extraction, wherein hexane is used to extract the lipids.

The extracted lipid is purified through a sequence of cleaning steps: degumming involving phosphoric acid addition, water washing, demetallization by silica addition, and bleaching with clay to eliminate additional metals and impurities. The resulting cake slurry from the purification process is directed to the wastewater treatment unit. The purified lipid is then sent to the hydrotreater, where, in the presence of hydrogen, it is transformed into hydrocarbon fuels. The hydrogen consumption rate is 1.7 wt% of the feed. Operating at 350 °C and 35 atm (Jones *et al.* 2014), the hydrotreating reactor carries out the conversion process.

Subsequently, the hydrocarbon fuels exiting the hydrotreater undergo fractionation and purification *via* distillation. Gas products are routed to the boiler, while any remaining aqueous materials are directed to the wastewater treatment unit. Key operating parameters are summarized in Table 1.

Modeling data inputs summarized in Table 1 and Table A2 represent optimal future case scenarios, particularly in the case of sugar and biofuel yields, which still need to be optimized at scale. While the sugar yield demonstrated at the bench-scale of nearly 80% of theoretical yield (Sundstrom *et al.* 2018; Magurudeniya *et al.* 2021) is close to the optimal sugar yield considered in this study, bisabolene yield, particularly utilizing the whole plant hydrolysate, is still in the very early stages of its development (Table A1). Further engineering of host microbes is required to achieve the desired titer, rate, and yield of bisabolene in the future. Additionally, the authors are not aware of any cell mass lipid to hydrocarbon fuel conversion process that has been demonstrated at bench scale. However, algal and plant lipids to hydrocarbon fuel conversion processes have been demonstrated (Jones *et al.* 2014).

The CO_2-to-methanol conversion process has been demonstrated at bench scale, and most recent works are focused on the selection of catalysts (Heracleous *et al.* 2023; Cai *et al.* 2023) that can enhance CO_2 conversion and methanol selectivity. Furthermore, researchers are conducting conversion of CO_2 in the liquid phase (Kothandaraman *et al.* 2022) instead of gas-phase CO_2 conversion into methanol. Research interests in these pathways are particularly focused on achieving higher CO_2 conversion and methanol selectivity, and lowering hydrogen loading. Therefore, future success in either cell mass or CO_2 utilization pathways could benefit bisabolene biorefinery to produce economically viable, carbon-negative bisabolene. Nonetheless, each conversion pathway, including bisabolene, methanol, and lipid-based hydrocarbon fuel production, offers ample opportunities for future research.

Table 1. Data Inputs Used to Develop Process Model in This Study

Parameters	Unit	Baseline Value	Range & Standard Deviation	Probability Distribution
Biomass Production & Supply (Baral *et al.* 2020; Gautam *et al.* 2023)				
Delivered Biomass Cost[α]	$/bdt	87.4	(65, 118.2)	Triangular
Carbon Footprint of Biomass[α]	$kgCO_{2e}$/bdt	95.6	(63.6, 144.7)	Triangular
Soil Carbon Sequestration[β]	$kgCO_{2e}$/bdt	-77.7	(-46, -192.6)	Triangular
Biomass Composition (Baral *et al.* 2019)				
Cellulose	wt%	40	(35.4, 44) & 5.31	Lognormal
Hemicellulose	wt%	29.8	(20.7, 30) & 3.79	Lognormal
Lignin	wt%	9.9	(8, 21) & 2.69	Lognormal
Biomass Deconstruction (Magurudeniya *et al.* 2021; Sundstrom *et al.* 2018)				
Solid Loading For Pretreatment	wt%	40	(30, 40)	Uniform
Ionic Liquid (IL) Loading	wt%	5	(2.5, 5)	Uniform
Enzyme Loading	mg/g-glucan	10	(7, 29.4)	Triangular
Solid Loading for Hydrolysis	wt%	25	(20, 30)	Uniform
Glucose Yield	%	95	(75.8, 99)	Uniform
Xylose Yield	%	90	(60.7, 99)	Uniform
Bioconversion (Humbird *et al.* 2011; Davis *et al.* 2018; Baral *et al.* 2023)				
Inoculum Loading	wt%	5	(4, 10)	Triangular
Bioconversion Time	h	36	(36, 72)	Uniform
Glucose-To-Bisabolene	wt%	28.5	(11.5, 29.4)	None
Xylose-To-Bisabolene	wt%	25.6	(10.3, 28.5)	None
Recovery & Separation (Baral *et al.* 2019; Jones *et al.* 2014)				
Bisabolene Recovery	wt%	98	(95, 99)	Uniform
IL Recovery	wt%	98	(95, 99)	Uniform
Wastewater Treatment (Humbird *et al.* 2011; Baral *et al.* 2023)				
Nutrient Loading	wt%	0.02	(0.01, 0.05)	Uniform
Organic Matter-To-Biogas	%	86	(86, 91)	Uniform
Onsite Energy & Utility (Humbird *et al.* 2011; Baral *et al.* 2023)				
Natural Gas Cost	$/kg	0.22	(0.1, 0.5) & 0.1	Normal
Water Cost	$/kg	0.0001	(0.0001, 0.00022)	Triangular
Cell Mass To Hydrocarbon (Koutinas *et al.* 2014; Jones *et al.* 2014)				
Hexane Loading	g/g-cell mass	0.3	(0.25, 5)	Triangular
Lipid Extraction	%	95	(85, 98)	Uniform
Microbial Oil Utilization	%	99	(95, 100)	Uniform
Hydrogen Cost[γ]	$/kg	2.8	(1, 6.0)	Triangular
Diesel Price[θ]	$/kg	0.6	(0.4, 0.7)	Triangular
CO_2-To-Methanol (Ramezan *et al.* 2007; Yang *et al.* 2020; Tan *et al.* 2015)				
Carbon Capture Efficiency	%	90	(60,95)	Triangular
Monoethanolamine Loading[Φ]	$molCO_2$/mol MEA	0.21	(0.1, 0.3)	Triangular
Monoethanolamine Concentration	wt%	30	(20, 50)	Triangular
Monoethanolamine Recycle Rate	%	96	(90, 99)	Triangular
Hydrogen Loading	wt%	0.137	(0.137, 0.137)	None
CO-To-Methanol	wt%	46	(46, 52)	Uniform

[α]Determined in this study by refining the model from the authors' prior work (Baral *et al.* 2020) and integrating a decent biomass yield of 22.4 bdt/ha (10 tons per acre).
[β]Collected from recent research (Gautam *et al.* 2023). Negative values mean net sequestration of carbon in soils.
[γ]Collected from recent studies (Bracci *et al.* 2023; Guerra *et al.* 2018).
[θ]The minimum, average, and maximum values over the past five years (E I A 2023).
[Φ]Collected from recent studies (Ramezan *et al.* 2007; Wang *et al.* 2023; Bravo *et al.* 2021).

Determining Production Cost

The methodology employed to determine the minimum selling price remained consistent with previous studies (Humbird *et al.* 2011; Davis *et al.* 2018). The process model was developed using SuperPro Designer, with material and energy balances conducted through the software's built-in functions for each unit operation. Sizing and quantities of process equipment were determined based on resulting material balance data.

The purchasing price of each process equipment was calculated by considering baseline price, baseline and new sizes, and the scaling exponent. Baseline size and equipment purchasing prices were sourced from recent publications (Humbird *et al.* 2011; Jones *et al.* 2014; Tan *et al.* 2015; Davis *et al.* 2018). This study's process model reflects changes in input parameters, illustrating their impacts on material and energy flows, as well as resulting capital and operating costs.

The capital cost was adjusted to the year 2022 using the plant cost index. Following the collection of capital and operating cost data from the developed process model, the discounted cash flow rate of return analysis (DCFROR) was conducted in Microsoft Excel. This analysis encompassed direct and indirect overhead cost factors consistent with the prior studies.

The DCFROR analysis aimed to determine the minimum selling price of bisabolene, considering a 10% internal rate of return (IRR) after taxes, a plant lifetime of 30 years, plant operating hours of 7920 hours (330 days/year and 24 hours/day), and an income tax rate of 21% (Davis *et al.* 2018; Gautam *et al.* 2023). Other economic evaluation parameters remained consistent with previous techno-economic studies.

The value of the Inflation Reduction Act (IRA) Sustainable Aviation Fuel (SAF) tax credit was estimated based on a recent notice issued by the Internal Revenue Service and Department of the Treasury (IRS 2023). SAF qualifies for a tax credit of $1.25 per gallon with a 50% reduction in GHG emissions. Moreover, an extra $0.01 per gallon is granted for each percentage point that exceeds the 50% reduction, capped at a maximum additional credit of $0.50 per gallon (IRS 2023). In addition to the SAF tax credit, the calculation also considered the low carbon fuel standard (LCFS) credit, which reflects California's most recent credit of $74 per metric ton of CO_2 (CARB 2023). Inclusion of these carbon reduction credits for cell mass and CO_2 utilization routes is purely hypothetical for the purposes of this study, as these systems have not been reviewed and approved as formal fuel production pathways.

Determining Lifecycle Greenhouse Gas Emissions

The lifecycle GHG footprint was determined using a previously developed input-output LCA model, which is detailed in a prior study (Neupane *et al.* 2017). Briefly, all direct and indirect materials and energy inputs, as well as their GHG emissions factors, were gathered from widely used databases such as the GREET model (GREET 2017), Ecoinvent (Ecoinvent 2017), and the U.S. LCI database (NREL 2012). The resulting GHG emissions factors generated from the input-output LCA model, harmonizing with the GREET LCA model are summarized in Table A3. Additionally, vital inputs to this life cycle assessment model comprised material and energy balanced data generated from the process model developed within this study.

The calculation of the onsite electricity credit involved accounting for the displacement of an equivalent amount of grid electricity (U.S. electricity mix). The same displacement methodology was employed to allocate GHG emissions credit from methanol and hydrocarbon fuels, presuming they displaced petroleum-derived methanol and

conventional diesel fuel. Furthermore, methanol combustion emissions are also considered as a credit, similar to hydrocarbon fuel, since it is derived from biogenic CO_2. The functional unit of 1 MJ of bisabolene was considered for analysis in this study.

Uncertainty Analysis

To quantify uncertainty, a single-point sensitivity analysis was conducted by taking into account the minimum and maximum values specified in Tables 1 and A1 for the input parameters. Furthermore, a two-point sensitivity analysis was conducted, concentrating on the two most influential input parameters and their respective ranges, as detailed in Table 1, to assess their combined impact on the selling price and carbon footprint of bisabolene.

Moreover, an overall determination of uncertainties concerning the selling price and GHG emissions across all chosen scenarios was made, inclusive of their corresponding input parameters. Probability distributions—including uniform, triangular, normal, and lognormal distributions outlined in Table 1—were utilized to model the variability in these input parameters (Baral *et al.* 2019). Five thousand Monte Carlo trials were run to generate the final probability distributions.

RESULTS AND DISCUSSION

Baseline Production Cost and Carbon Footprint

Figure 2(A) depicts the capital investment of various biorefinery configurations considered in this study. Bioconversion (21%), wastewater treatment (18%), and onsite energy generation units (31%) are the primary contributors to the total capital investment of the baseline biorefinery with no cell mass lipids and CO_2 utilizations. Importantly, diverting microbial lipids to the hydrocarbon fuel production unit reduces the capital cost of the onsite energy generation unit by 8.4%, consequently reducing potentially harmful air pollutants (Eberle *et al.* 2017).

Utilizing both cell mass and CO_2 further increases the capital investment by 1.7 times relative to the conventional biorefinery. The capital cost of CO_2 capture and utilization, as well as cell mass upgrading units, are evident additions. Indeed, it is noteworthy that this biorefinery configuration generates 63% higher electricity than the conventional biorefinery, even without sourcing external natural gas. This increase is mainly attributed to unconverted CO and lost hydrogen from the CO_2 utilization process being directed to the boiler. However, it is important to acknowledge that this enhanced electricity generation comes at a cost, as it concurrently increases the capital cost of boilers and turbines by 73% (Fig. 2A). This trade-off between increased electricity output and higher capital cost underscores the complexity of optimizing biorefinery configurations for both efficiency and economic considerations. This also emphasizes the importance of developing an efficient conversion of CO_2 to CO to provide an alternative energy source for the boiler.

Developing a self-powered biorefinery with cell mass and CO_2 utilization results in a capital- and energy-intensive facility that also demands a large amount of natural gas, thereby increasing the carbon footprint. This suggests that such biorefineries may either need supplemental electricity from the grid, which can help reduce the overall carbon footprint. However, to effectively achieve this reduction, it is essential to build these biorefineries in locations where renewable electricity can be generated onsite or where renewable electricity constitutes a significant fraction of the grid's total electricity.

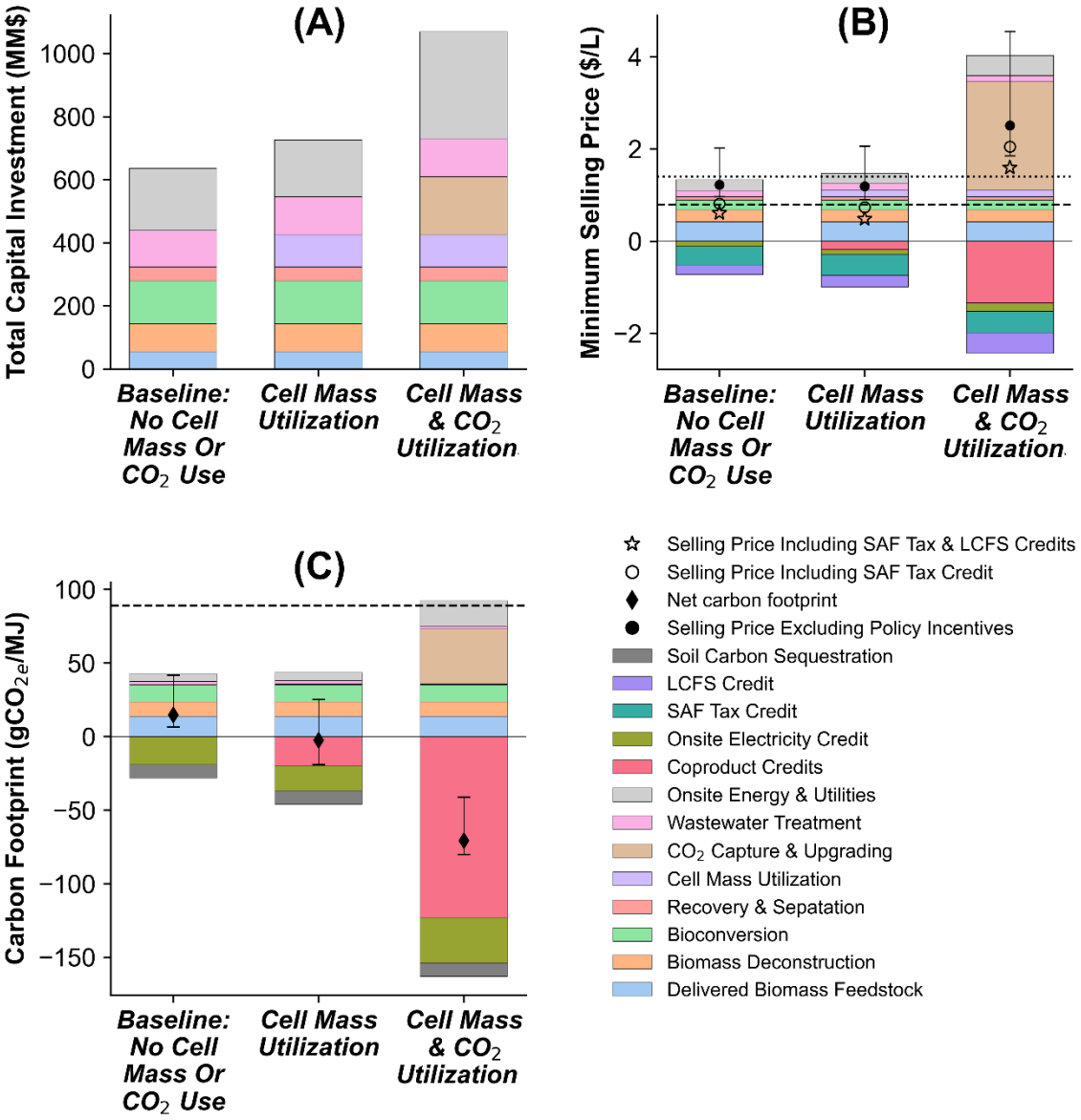

Fig. 2. Capital investment of bisabolene biorefinery under three different configurations (A), along with the associated minimum selling prices (B) and greenhouse gas emissions (C). The horizontal dashed lines represent the baseline price in 2050 (2022$) of $0.78/L (EIA 2023) and greenhouse gas emissions of conventional jet fuel of 89 gCO_{2e}/MJ (GREET 2017). The horizontal dotted line represents the price of conventional jet fuel in 2050 (2022$) under a high oil price scenario of $1.4/L (EIA 2023). Sensitivity bars represent the impacts of a ±15% variation in baseline values of the most influential input parameters (Figures A1 and A2), except for bisabolene yield, which was set at 90% of the theoretical yield.

Figure 2(B) illustrates the minimum selling price of bisabolene, with significant contributions from delivered biomass feedstock, enzyme, and ionic liquid used in biomass deconstruction, nitrogen sources (ammonia, corn steep liquor, and ammonium phosphate) employed in bioconversion, and the capital recovery cost associated with bioconversion, wastewater treatment, and onsite energy generation units. The conversion of cell mass lipids to hydrocarbon fuels can cover the additional operating costs required for the process, resulting in a reduction of the minimum selling price by 2.7% relative to the

conventional biorefinery. The upgrading of cell mass is a capital-intensive process, being a primary contributor to the operating cost at this stage, along with the costs of hexane, hydrotreating catalyst, and hydrogen.

While the CO_2 capture and upgrading process is capital-intensive, a significant portion of the operating cost (87%) is attributed to material costs. Hydrogen accounts for 72.5% of this cost, MEA contributes 27.4%, and the remaining 0.1% is attributed to catalysts. Variations in MEA concentration and loading rate reported in the literature (Ramezan *et al.* 2007; Tan *et al.* 2015) indicate room for improvement. However, the amount of hydrogen required (nearly 14 g per 100 g of CO_2) for the selective catalytic upgrading of CO_2 to methanol is unavoidable.

This underscores the need for low-cost renewable hydrogen, which poses a challenge considering recent estimates of hydrogen production costs from renewable resources in California, Texas, and New York in the range of $2.02 to 2.88/kg (Bracci *et al.* 2023). There is a possibility of achieving the near-term hydrogen production cost target of $2/kg; however, substantial technological improvements are required to reach the long-term hydrogen production cost target of $1/kg (DOE 2023), which is 2.8 times lower than the hydrogen price considered in this work.

A supply of low-cost hydrogen at $1/kg has the potential to reduce the baseline selling price of bisabolene by 38%, bringing it to a level sufficient for cost-parity with the conventional jet fuel price in 2050 at $0.79/L (2022$) (EIA 2023). This may be more achievable in the near term once policy incentives at the Federal and state level are factored in. However, inclusion of such policy incentives are beyond the scope of this study. Notably, bisabolene produced in both a conventional biorefinery and a biorefinery with cell mass lipids diverted to hydrocarbon fuel production has the potential to be priced below the conventional jet fuel, even in the absence of any policy support, especially under high oil price scenarios.

Appropriately selected biorefinery configurations, whether utilizing only cell mass lipids or incorporating both microbial lipids and CO_2 utilization, have the potential to achieve a substantial GHG emissions reduction, ranging from 84% to 180% relative to petroleum (Fig. 2C). This surpasses the challenge of achieving a 60% reduction relative to petroleum, underscoring the effectiveness of these configurations in substantially mitigating GHG emissions. Importantly, carbon-negative bisabolene can be produced by redirecting cell mass lipids to hydrocarbon fuel. In scenarios involving both cell mass lipids and CO_2 utilization, the GHG emissions of bisabolene contribute to a large CO_2 emissions reduction compared to the baseline biorefinery. It is crucial to note that in this process, the hydrogen used is assumed to be generated from renewable sources. However, in the scenario with both cell mass and CO_2 utilization, utilizing hydrogen generated from fossil natural gas would result in positive GHG emissions for bisabolene, with only a 30% reduction relative to conventional jet fuel. This highlights the importance of producing low-cost renewable hydrogen for carbon-negative renewable aviation fuels production in the future.

The main driver of GHG emissions reduction in processes involving either cell mass lipids or both microbial lipids and CO_2 utilizations is the accumulation of GHG emissions displacement credits from hydrocarbon fuel. Additionally, CO_2 utilization provides credits from methanol and electricity generated from the unutilized CO and hydrogen lost from the process. These credits, when combined with GHG emissions credits from lignin-derived electricity, prove to be adequate for offsetting GHG emissions from key sources. These sources include delivered biomass, enzymes, ionic liquid, electricity

primarily required for bioconversion, CO_2 compression from near 1 bar to the reactor operating pressure of 51 bar, and utilities, particularly in the generation of chilled water.

This result underscores the importance of having a co-product that displaces its petroleum counterpart for GHG emissions reduction. However, achieving substantial cost reduction necessitates the production of a high-value co-product.

Uncertainty in Production Costs and GHG Emissions

Figure 3 demonstrates the uncertainty in minimum selling price and GHG emissions. The major sources of this uncertainty and their individual impact on bisabolene selling price and GHG emissions are documented in APPENDIX Figs. A1 and A2. Variabilities present in key input parameters (Figs. A1 and A2) have the potential to alter either the amount of product and co-product generated, or the energy and process chemicals required, or both, resulting in variations in both production cost and GHG emissions.

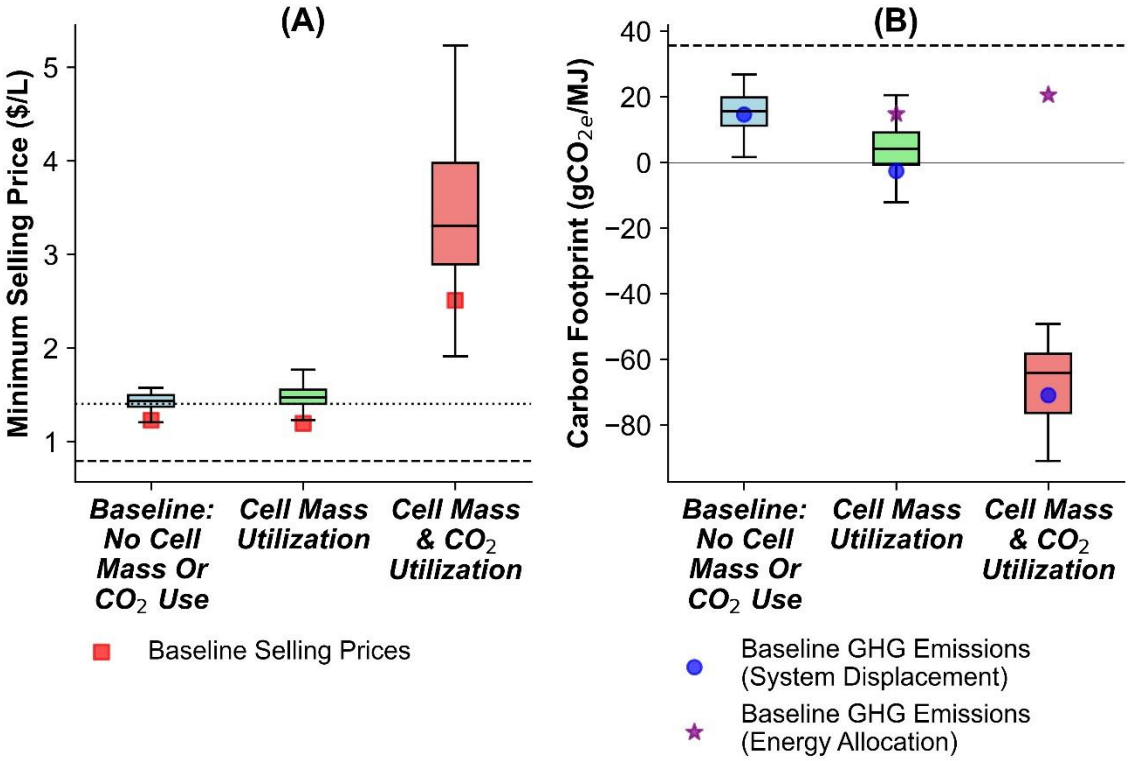

Fig. 3. Uncertainty associated with selling price (A) and greenhouse gas emissions (B) of bisabolene. The baseline values and variabilities present in input parameters are presented in Table 1. For this analysis, the bisabolene yield was set at 90% of the theoretical yield. The horizontal dashed lines represent the baseline price in 2050 (2022$) of $0.78/L (EIA 2023) and targeted greenhouse gas emissions reduction of 60 % relative to conventional jet fuel. The horizontal dotted line represents the price of conventional jet fuel in 2050 (2022$) under a high oil price scenario of $1.4/L (EIA 2023).

A wide range of variability considered in hydrogen price at the reactor throat, ranging from $1 to 6/kg, stands out as the single largest source of uncertainty in bisabolene selling price, particularly in the scenario involving both CO_2 and cell mass lipid utilizations. In this context, a price of up to $6/kg is considered, as it is likely in different regions in the U.S. (Bracci *et al.* 2023), while the targeted future price is set considerably lower at $1/kg. In the scenario involving only cell mass upgrading, the process exhibits less uncertainty despite a large variability in hydrogen price due to the relatively small amount of hydrogen required for the cell mass lipids upgrading process, specifically at 1.7 wt%. This suggests that choosing pathways (Do *et al.* 2022) that necessitate a smaller amount of hydrogen for converting CO_2 into valuable fuels and chemicals is crucial, even when substantial reductions in hydrogen prices may not be feasible in the future.

The variability in amine loading is another substantial source of uncertainty in the scenario involving both microbial lipids and CO_2 utilizations, while it is not applicable for other scenarios. This highlights the importance of finely tuning amine and its concentration for effective CO_2 capture. The process parameters considered for the static model are mostly optimal for analysis in this study, indicating a very low probability of achieving a selling price resulting from the static model (Fig. 3A). Any changes in parameters are likely to increase the selling price of bisabolene. However, variations in input parameters are likely to decrease GHG emissions (Fig. 3B). For instance, an increase in lignin content in biomass, which is unlikely to reduce the selling price of bisabolene (APPENDIX Fig. A1), reduces GHG emissions by increasing GHG emission credits obtained from lignin-derived electricity.

For the combined system evaluated in this study, when the process is less efficient and generates more cell mass or CO_2, coproducts generated from them substantially reduce GHG emissions (Fig. A2) by displacing their petroleum counterparts. However, this is not desirable from an economic or carbon conversion efficiency standpoint. Alternatively, efficiently utilizing both CO_2 and cell mass provides substantial GHG emissions reduction credits and is important for expanding future carbon-negative biofuels policies. While the system displacement method leads to a large negative GHG emissions with multiple coproducts, future biofuel policies could explore alternative allocation methods for factoring in GHG emissions credits of coproducts. For instance, the energy-based allocation method results in positive GHG emissions for bisabolene (Fig. 3B) similar to the baseline biorefinery configuration, which does not utilize cell mass and CO_2. Thus, the focus of scientific research should be on maximizing both products and co-products and selecting an appropriate product mix to gain large GHG emissions reduction benefits.

Bisabolene and Cell Mass Yields to Achieve Cost Parity

The genome-scale metabolic analysis model developed in this work reveals that 48 to 62 wt% of CO_2 is formed in the bioconversion process. This occurs irrespective of whether the remaining carbon sources are directed solely towards cell mass or distributed between cell mass and bisabolene. This formation depends on the ratio of carbon sources, including glucose and xylose present in the bioreactor. The generation of cell mass is inversely related to the formation of the product (see APPENDIX, Fig. A3). There is a possibility of diverting most carbon sources into the product or cell mass beyond what is reported in this work through genetic engineering or pathway modifications, but this aspect is beyond the scope of this study.

Our model considers microbial growth in the seed reactor utilizing 10 wt% hydrolysate, where most of the sugars are assumed to be diverted into cell mass. The results

presented in Fig. 4 combine the cell mass generated in the seed reactors and in the main bioreactor, which is modeled based on the genome-scale metabolic modeling results presented in Fig. A3.

In the scenario where only cell mass lipids are converted to hydrocarbon fuel (Fig. 4A), bisabolene selling could reach cost parity with conventional jet fuel (high oil price scenario) without any policy support when bisabolene yield reaches 54% of the theoretical yield (30 g per 100 g of sugars), with 38 wt% cell mass formed. The currently reported bisabolene yield from biomass hydrolysate is approximately 8% of the theoretical yield (Table A1). To reach cost parity with the baseline conventional jet fuel price, policy incentives are required. With only carbon tax credit, reaching cost parity with the baseline conventional jet fuel price requires a bisabolene yield of 70% of the theoretical yield, with 29 wt% cell mass formed. Including both carbon tax credit and LCFS credits, only 30% of the theoretical bisabolene yield is required, with 48 wt% of cell mass formed.

The results indicate that cost-effective low-carbon biofuel can be produced without substantial research investment in achieving near theoretical biofuel yield. However, it requires appropriate selection of the product and cell mass ratio and microbes that contain above 60% lipid based on dry cell mass, such as *R. toruloides*. In contrast, when both cell mass lipid and CO_2 are utilized (Fig. 4B), it is challenging to reach cost parity with conventional jet fuel, even if the theoretical yield of bisabolene is achieved and fully incorporates policy incentives. As discussed earlier, this biorefinery requires low-cost hydrogen to produce cost-effective bisabolene.

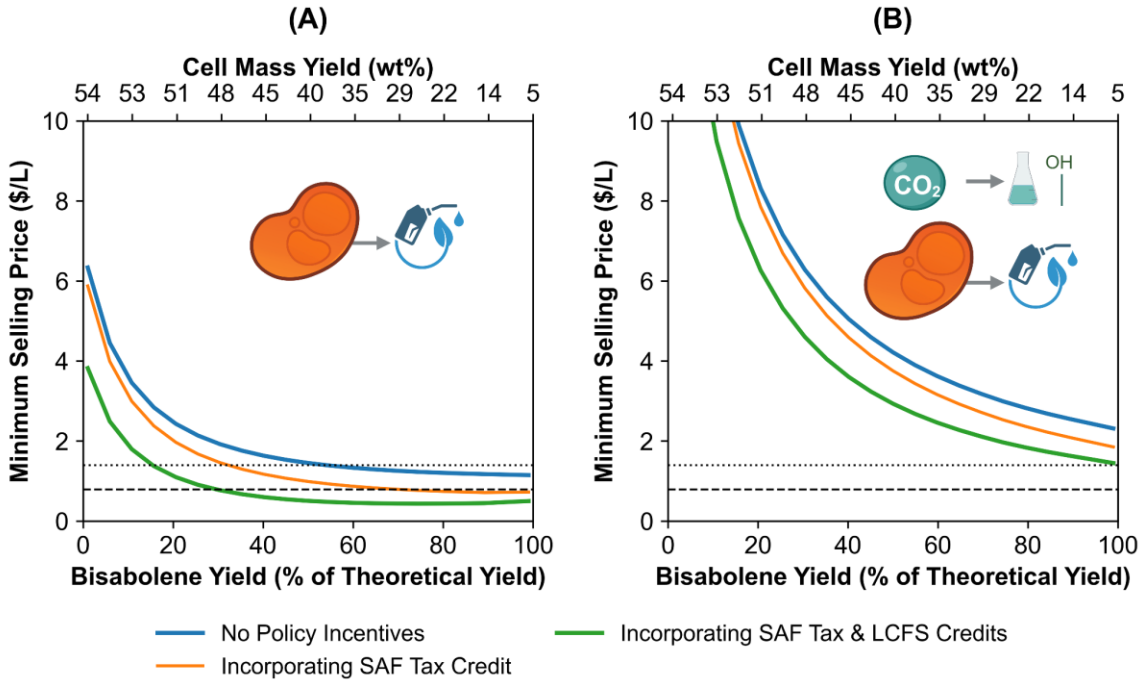

Fig. 4. Selling price of bisabolene in relation to its yield and the corresponding cell mass yield with a biorefinery only utilizing cell mass lipids (A) and utilizing both microbial lipids and CO_2 (B). All policy incentives included are based on estimates from this study and may deviate from fully compliant carbon intensities. The horizontal dashed and dotted lines, respectively, represent the price of conventional jet fuel in 2050 (2022$) under the baseline scenario of $0.78/L and the high oil price scenario of $1.4/L (EIA 2023).

Process Bottlenecks and Optimization Opportunities

To make both cell mass lipids and CO_2 utilization processes cost-effective, in addition to requiring low-cost hydrogen, fine-tuning of MEA loading is necessary. At a hydrogen price of $1/kg and fully incorporating the SAF tax credit and LCFS credits, reaching cost parity with the baseline conventional jet fuel price of $0.79/L requires an MEA loading of more than 0.18 mol CO_2/mol MEA, meaning a lesser amount of MEA per mol of CO_2 (Fig. 5A). For the high oil price scenario, to achieve cost parity at a hydrogen price of $2/kg and fully incorporating policy incentives, an MEA loading of at least 0.16 mol CO_2/mol MEA is required (Fig. 5A). While these MEA loadings are reasonable to capture more than 90% CO_2 (Ramezan *et al.* 2007), reducing MEA loading could impact CO_2 capture efficiency. The results also show that even at a lower MEA loading, exceeding a hydrogen price above $3.2/kg would be very challenging to reach cost parity with conventional jet fuel, even with a high oil price scenario and fully incorporating policy incentives (Fig. 5A). This warrants innovative solutions to make CO_2 utilization systems economically viable.

One potential approach involves CO_2 capture using the solvent N-(2-EthoxyEthyl)-3-Mor-pholinoPropan-1-Amine (2-EEMPA) and pumping the entire condensed phase (2-EEMPA-CO2-H2O mixture) to a methanol synthesis reactor (Kothandaraman *et al.* 2022). In this reactor, methanol is produced through the hydrogenation of the condensed phase, facilitated by a 5wt% Pt/TiO_2 catalyst and hydrogen (Kothandaraman *et al.* 2022), contrasting with the gas phase hydrogenation of CO_2 considered in the baseline analysis of this study. This system exhibits the potential to reduce both capital costs and energy consumption. The present findings indicate that substituting the baseline methanol synthesis, employing gas phase hydrogen, with the state-of-the-art condensed phase hydrogenation system can decrease GHG emissions from bisabolene by 1.6 times. The reduction in GHG emissions is mainly attributed to GHG emission credits from co-products, including alcohols, methane, and ethane. However, current bench-scale experimental data (Kothandaraman *et al.* 2022) results in 42% higher selling price of bisabolene. This increase is primarily due to the relatively expensive catalyst, its higher loading, and the low selectivity of methanol. To further enhance cost-effectiveness, the condensed phase hydrogenation process requires refinement in CO2 conversion, aiming for higher methanol selectivity at lower catalyst and hydrogen loadings.

Another potential solution is to generate onsite renewable hydrogen from water electrolysis and fully utilize oxygen generated in the process. Oxygen can be used for aeration in the bioreactor and to burn fuel, mainly lignin, in the boiler. For a typical biorefinery utilizing 2000 bdt of biomass per day, fully generating onsite hydrogen required for cell mass lipids upgrading and CO_2 to methanol conversion also generates sufficient oxygen for the biorefinery. Using oxygen in the bioreactor and boiler not only generates concentrated CO_2 but also reduces the electricity consumption of the biorefinery. The largest decrease in electricity consumption was observed in the bioreactor, reaching a 63% reduction, when air was replaced with oxygen for aeration.

Concentrated CO_2 could be directly delivered to the H_2S removal unit and subsequently to the methanol synthesis reactor, potentially eliminating the amine-based CO_2 capture system. The bisabolene production cost results of this system are presented in Fig. 5(B). The results suggest that achieving near theoretical bisabolene yield, the selling price of bisabolene reaches cost parity with the baseline conventional jet fuel price of $0.79/L at a hydrogen cost of $2.4/kg, incorporating both SAF tax credit and LCFS credits. For the high oil price scenario, the bisabolene selling price reaches cost parity with

conventional jet fuel at a hydrogen price of $3.4/kg. Beyond a hydrogen price of $3.4/kg, this system may face challenges in producing economically viable bisabolene without further technological improvements.

Selecting suitable hosts containing high lipids does not necessitate pushing engineering efforts to achieve the theoretical yield of biofuels. For instance, achieving a bisabolene yield of at least 80% of the theoretical yield is essential for generating economically viable bisabolene, contingent upon policy support and producing renewable hydrogen in the range of $2.2 to $3.1 per kg. Future research could explore an appropriate combination of CO_2, cell mass, and biofuel yield to maximize economic gain and lower greenhouse gas emissions.

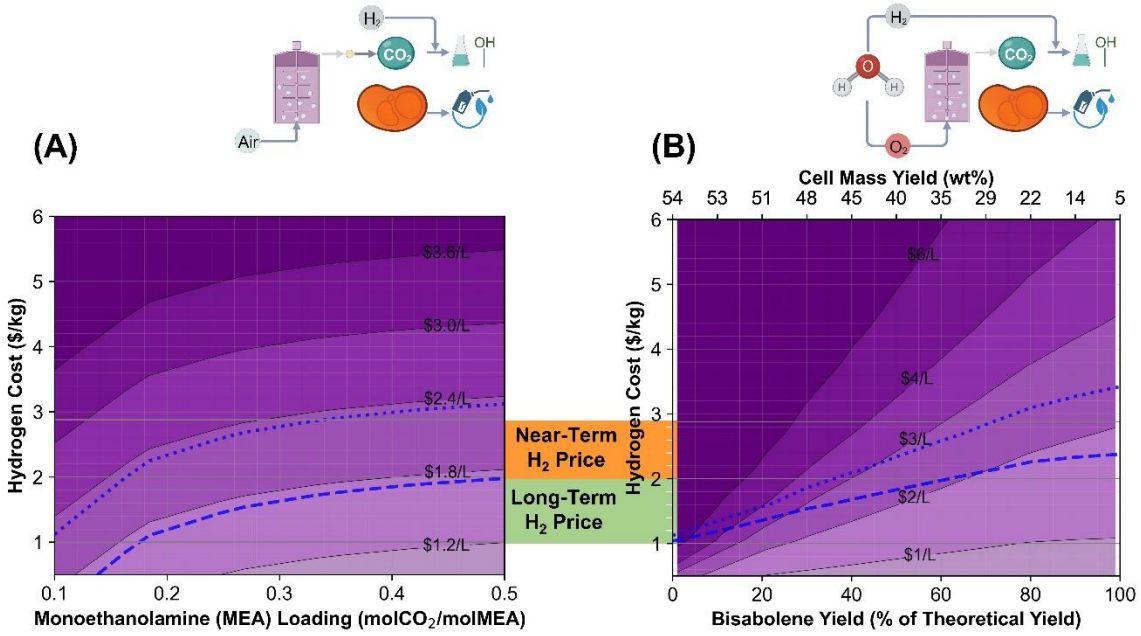

Fig. 5. Influence of the two primary parameters in a conventional biorefinery using air for aeration in a bioreactor and sourcing renewable hydrogen (A), versus an alternative biorefinery employing onsite water electrolysis and fully utilizing both hydrogen and oxygen (B). The dashed and dotted lines represent cost parity with conventional jet fuel under the baseline and high oil price scenarios, respectively, incorporating SAF tax credit and LCFS credits.

CONCLUSIONS

1. Combining cell mass lipids and CO_2 utilization produces carbon-negative bisabolene; however, achieving cost parity with conventional jet fuel depends on overcoming the crucial process bottleneck of low-cost hydrogen availability, requiring renewable hydrogen production at $2 to 3/kg or lower contingent on bisabolene yield success and the availability of policy incentives such as SAF tax credit and LCFS credits.
2. Meeting onsite hydrogen requirements with water electrolysis not only provides adequate oxygen for aeration and combustion but also, by replacing air with oxygen, reduces biorefinery energy consumption and yields concentrated CO_2, with the most substantial 63% reduction in electricity consumption found in the bioconversion stage.

3. To achieve cost parity with conventional jet fuel, the amine-based carbon capture system requires an amine loading of 0.16 to 0.18 mol CO_2/mol MEA, contingent on hydrogen availability at $1 to 2 per kg and policy incentives.
4. Utilizing solely microbial lipids for hydrocarbon fuel in a conventional bisabolene biorefinery produces carbon-negative biofuels, and achieving cost parity with conventional jet fuel requires a minimum of 30% of the theoretical yield of bisabolene, considering both SAF tax credit and LCFS credits, and 70% of the theoretical yield of bisabolene, factoring in only SAF tax credit. This configuration has the potential to generate economically viable bisabolene without the need for any policy support
5. Diverting microbial lipids to hydrocarbon fuel production instead of burning them in a boiler reduces the capital cost of the boiler and turbine by 8.4%, with the additional potential to decrease harmful air pollutants.

ACKNOWLEDGMENTS

This work was part of the DOE Joint BioEnergy Institute (http://www.jbei.org) supported by the U.S. Department of Energy, Office of Science, Office of Biological and Environmental Research, through contract DE-AC02-05CH11231 between Lawrence Berkeley National Laboratory and the U.S. Department of Energy. This study was also supported by the U.S. Department of Energy, Energy Efficiency and Renewable Energy, Bioenergy Technologies Office. The United States Government retains and the publisher, by accepting the article for publication, acknowledges that the United States Government retains a nonexclusive, paid-up, irrevocable, worldwide license to publish or reproduce the published form of this manuscript, or allow others to do so, for United States Government purposes. Elements of the graphical abstract and Figures 1, 4, and 5 were created with BioRender.com.

Conflicts of Interest

N.R.B. and B.A.S. have a financial interest in Erg Bio. B.A.S. has a financial interest in Caribou Biofuels and Illium Technologies. C.D.S. has a financial interest in Cyklos Materials.

REFERENCES CITED

Aden, A., Ruth, M., Ibsen, K., Jechura, J., Neeves, K., Sheehan, J., Wallace, B., Montague, L., Slayton, A., and Lukas, J. (2002). *Lignocellulosic Biomass to Ethanol Process Design and Economics Utilizing Co-Current Dilute Acid Prehydrolysis and Enzymatic Hydrolysis for Corn Stover*, National Renewable Energy Laboratory (NREL), Golden, CO. DOI: 10.2172/15001119

Aggarwal, N., Pham, H. L., Ranjan, B., Saini, M., Liang, Y., Hossain, G. S., Ling, H., Foo, J. L., and Chang, M. W. (2023). "Microbial engineering strategies to utilize waste feedstock for sustainable bioproduction," *Nature Reviews Bioengineering*. DOI: 10.1038/s44222-023-00129-2

Alonso-Gutierrez, J., Kim, E.-M., Batth, T. S., Cho, N., Hu, Q., Chan, L. J. G., Petzold, C. J., Hillson, N. J., Adams, P. D., Keasling, J. D., Garcia Martin, H., and Lee, T. S.

(2015). "Principal component analysis of proteomics (PCAP) as a tool to direct metabolic engineering," *Metabolic Engineering* 28, 123-133. DOI: 10.1016/j.ymben.2014.11.011

Banerjee, D., Eng, T., Lau, A. K., Sasaki, Y., Wang, B., Chen, Y., Prahl, J. P., Singan, V. R., Herbert, R. A., Liu, Y., and Tanjore, D. (2020). "Genome-scale metabolic rewiring improves titers rates and yields of the non-native product indigoidine at scale," *Nature Communications* 11(1), article 5385. DOI: 10.1038/s41467-020-19171-4

Baral, N. R., Banerjee, D., Mukhopadhyay, A., Simmons, B. A., Singer, S. W., and Scown, C. D. (2023). "Economic and environmental trade-offs of simultaneous sugar and lignin utilization for biobased fuels and chemicals," *ACS Sustainable Chemistry & Engineering* 12(7), 2563-2576. DOI: 10.1021/acssuschemeng.3c05541

Baral, N. R., Dahlberg, J., Putnam, D., Mortimer, J. C., and Scown, C. D. (2020). "Supply cost and life-cycle greenhouse gas footprint of dry and ensiled biomass sorghum for biofuel production," *ACS Sustainable Chemistry & Engineering* 8(42), 15855-15864. DOI: 10.1021/acssuschemeng.0c03784

Baral, N. R., Kavvada, O., Mendez-Perez, D., Mukhopadhyay, A., Lee, T. S., Simmons, B. A., and Scown, C. D. (2019a). "Techno-economic analysis and life-cycle greenhouse gas mitigation cost of five routes to bio-jet fuel blendstocks," *Energy & Environmental Science* 12(3), 807-824. DOI: 10.1039/C8EE03266A

Baral, N. R., Sundstrom, E. R., Das, L., Gladden, J. M., Eudes, A., Mortimer, J., Singer, S. W., Mukhopadhyay, A., and Scown, C. D. (2019b). "Approaches for more efficient biological conversion of lignocellulosic feedstocks to biofuels and bioproducts," *ACS Sustainable Chemistry & Engineering* 7(10), 9062-9079. DOI: 10.1021/acssuschemeng.9b01229

Bracci, J. M., Sherwin, E. D., Boness, N. L., and Brandt, A. R. (2023). "A cost comparison of various hourly-reliable and net-zero hydrogen production pathways in the United States," *Nature Communications* 14(1), article 7391. DOI: 10.1038/s41467-023-43137-x

Bravo, J., Drapanauskaite, D., Sarunac, N., Romero, C., Jesikiewicz, T., and Baltrusaitis, J. (2021). "Optimization of energy requirements for CO_2 post-combustion capture process through advanced thermal integration," *Fuel* 283, article 118940. DOI: 10.1016/j.fuel.2020.118940

Butcher, M. G., Meyer, P. A., Hallen, R. T., Albrecht, K. O., Clayton, C. K., Polikarpov, E., Rappe, K. G., Jones, S. B., and Magnuson, J. K. (2018). "Fungal metabolites as precursors to renewable transportation fuels," *Fuel* 215, 123-141. DOI: 10.1016/j.fuel.2017.10.052

Cai, D., Cai, Y., Tan, K. B., and Zhan, G. (2023). "Recent advances of indium oxide-based catalysts for CO_2 hydrogenation to methanol: Experimental and theoretical," *Materials* 16(7), article 2803. DOI: 10.3390/ma16072803

CARB. (2023). "Monthly LCFS Credit Transfer Activity Reports," (https://ww2.arb.ca.gov/resources/documents/monthly-lcfs-credit-transfer-activity-reports), Accessed 9 January 2024.

Davis, R. E., Grundl, N. J., Tao, L., Biddy, M. J., Tan, E. C., Beckham, G. T., Humbird, D., Thompson, D. N., and Roni, M. S. (2018). *Process design and economics for the conversion of lignocellulosic biomass to hydrocarbon fuels and coproducts: 2018 biochemical design case update; biochemical deconstruction and conversion of biomass to fuels and products via integrated biorefinery pathways*, National

Renewable Energy Laboratory (NREL), Golden, CO (United States). DOI: 10.2172/1483234

Dinh, H. V., Suthers, P. F., Chan, S. H. J., Shen, Y., Xiao, T., Deewan, A., Jagtap, S. S., Zhao, H., Rao, C. V., Rabinowitz, J. D., and Maranas, C. D. (2019). "A comprehensive genome-scale model for *Rhodosporidium toruloides* IFO0880 accounting for functional genomics and phenotypic data," *Metabolic Engineering Communications* 9, article e00101. DOI: 10.1016/j.mec.2019.e00101

DOE. (2023). "Hydrogen production: Electrolysis," (https://www.energy.gov/eere/fuelcells/hydrogen-production-electrolysis), Accessed 13 January 2024.

Do, T. N., You, C., and Kim, J. (2022). "A CO_2 utilization framework for liquid fuels and chemical production: Techno-economic and environmental analysis," *Energy & Environmental Science* 15(1), 169-184. DOI: 10.1039/D1EE01444G

Eberle, A., Bhatt, A., Zhang, Y., and Heath, G. (2017). "Potential air pollutant emissions and permitting classifications for two biorefinery process designs in the United States," *Environmental Science & Technology* 51(11), 5879-5888. DOI: 10.1021/acs.est.7b00229

Ecoinvent. (2017). "Ecoinvent database," (https://ecoinvent.org/the-ecoinvent-database/), Accessed 22 January 2024.

EIA. (2023). "Petroleum and Other Liquids Prices," (https://www.eia.gov/outlooks/aeo/data/browser/#/?id=12-AEO2023&region=0-0&cases=ref2023~highmacro~lowmacro~highprice~lowprice~highogs~lowogs~highZTC~lowZTC~aeo2022ref&sourcekey=0), Accessed 11 January 2024.

Ferraz, C. A., Leferink, N. G. H., Kosov, I., and Scrutton, N. S. (2021). "Isopentenol utilization pathway for the production of linalool in *Escherichia coli* using an improved bacterial linalool/nerolidol synthase," *Chembiochem* 22(13), 2325-2334. DOI: 10.1002/cbic.202100110

Gautam, S., Baral, N. R., Mishra, U., and Scown, C. D. (2023). "Impact of bioenergy feedstock carbon farming on sustainable aviation fuel viability in the United States," *Proceedings of the National Academy of Sciences of the United States of America* 120(51), article e2312667120. DOI: 10.1073/pnas.2312667120

GREET. (2017). "Energy systems and infrastructure analysis," (https://greet.anl.gov/), accessed 22 January 2024.

Guerra, O. J., Eichman, J., Hodge, B.-M., and Kurtz, J. (2018). *Cost-Competitive Electrolysis-Based Hydrogen Under Current US Electric Utility Rates*, National Renewable Energy Laboratory, Golden, CO, USA.

Harris, K., Grim, R. G., Huang, Z., and Tao, L. (2021). "A comparative techno-economic analysis of renewable methanol synthesis from biomass and CO_2: Opportunities and barriers to commercialization," *Applied Energy* 303, article 117637. DOI: 10.1016/j.apenergy.2021.117637

Heracleous, E., Koidi, V., and Lappas, A. A. (2023). "Experimental investigation of sorption-enhanced CO_2 hydrogenation to methanol," *ACS Sustainable Chemistry & Engineering* 11(26), 9684-9695. DOI: 10.1021/acssuschemeng.3c01424

Huang, Y., Ye, Z., Wan, X., Yao, G., Duan, J., Liu, J., Yao, M., Sun, X., Deng, Z., Shen, K., Jiang, H., and Liu, T. (2023). "Systematic mining and evaluation of the sesquiterpene skeletons as high energy aviation fuel molecules," *Advanced Science (Weinheim, Baden-Wurttemberg, Germany)* 10(23), article e2300889. DOI: 10.1002/advs.202300889

Humbird, D., Davis, R., Tao, L., Kinchin, C., Hsu, D., Aden, A., Schoen, P., Lukas, J., Olthof, B., Worley, M., Sexton, D., and Dudgeon, D. (2011). *Process Design and Economics for Biochemical Conversion of Lignocellulosic Biomass to Ethanol: Dilute-Acid Pretreatment and Enzymatic Hydrolysis of Corn Stover*, National Renewable Energy Laboratory (NREL), Golden, CO (United States). DOI: 10.2172/1013269

Huntington, T., Cui, X., Mishra, U., and Scown, C. D. (2020). "Machine learning to predict biomass sorghum yields under future climate scenarios," *Biofuels, Bioproducts and Biorefining* 14(3), 566-577. DOI: 10.1002/bbb.2087

IRS. (2023). "Sustainable Aviation Fuel Credit," (https://www.irs.gov/pub/irs-drop/n-24-06.pdf?utm_medium=email&utm_source=govdelivery), Accessed 9 January 2024.

Jones, S. B., Zhu, Y., Anderson, D. B., Hallen, R. T., Elliott, D. C., Schmidt, A. J., Albrecht, K. O., Hart, T. R., Butcher, M. G., Drennan, C., Snowden-Swan, L. J., Davis, R., and Kinchin, C. (2014). *Process Design and Economics for the Conversion of Algal Biomass to Hydrocarbons: Whole Algae Hydrothermal Liquefaction and Upgrading*, Pacific Northwest National Laboratory (PNNL), Richland, WA (United States). DOI: 10.2172/1126336

Kang, A., Mendez-Perez, D., Goh, E.-B., Baidoo, E. E. K., Benites, V. T., Beller, H. R., Keasling, J. D., Adams, P. D., Mukhopadhyay, A., and Lee, T. S. (2019). "Optimization of the IPP-bypass mevalonate pathway and fed-batch fermentation for the production of isoprenol in *Escherichia coli*," *Metabolic Engineering*, 56, 85-96. DOI: 10.1016/j.ymben.2019.09.003

Keller, C. L., Walkling, C. J., Zhang, D. D., Baldwin, L. C., Austin, J. S., and Harvey, B. G. (2023). "Designer biosynthetic jet fuels derived from isoprene and α-olefins," *ACS Sustainable Chemistry & Engineering* 11(10), 4030-4039. DOI: 10.1021/acssuschemeng.2c05297

Kim, J., Coradetti, S. T., Kim, Y.-M., Gao, Y., Yaegashi, J., Zucker, J. D., Munoz, N., Zink, E. M., Burnum-Johnson, K. E., Baker, S. E., Simmons, B. A., Skerker, J. M., Gladden, J. M., and Magnuson, J. K. (2020). "Multi-omics driven metabolic network reconstruction and analysis of lignocellulosic carbon utilization in *Rhodosporidium toruloides*," *Frontiers in Bioengineering and Biotechnology* 8, article 612832. DOI: 10.3389/fbioe.2020.612832

Kim, J., Coradetti, S. T., Kim, Y. M., Gao, Y., Yaegashi, J., Zucker, J. D., Munoz, N., Zink, E. M., Burnum-Johnson, K. E., Baker, S. E., Simmons, B. A., Skerker, J. M., Gladden, J. M., and Magnuson, J. K. (2021). "Multi-omics driven metabolic network reconstruction and analysis of lignocellulosic carbon utilization in *Rhodosporidium toruloides*," *Frontiers in Bioengineering and Biotechnology* 8, article 612832. DOI: 10.3389/fbioe.2020.612832

Kim, J., and Lee, T. S. (2023). "Enhancing isoprenol production by systematically tuning metabolic pathways using CRISPR interference in *E. coli*," *Frontiers in Bioengineering and Biotechnology* 11, article 1296132. DOI: 10.3389/fbioe.2023.1296132

Kirby, J., Geiselman, G. M., Yaegashi, J., Kim, J., Zhuang, X., Tran-Gyamfi, M. B., Prahl, J.-P., Sundstrom, E. R., Gao, Y., Munoz, N., Burnum-Johnson, K. E., Benites, V. T., Baidoo, E. E. K., Fuhrmann, A., Seibel, K., Webb-Robertson, B.-J. M., Zucker, J., Nicora, C. D., Tanjore, D., Magnuson, J. K., and Gladden, J. M. (2021). "Further engineering of *R. toruloides* for the production of terpenes from lignocellulosic biomass," *Biotechnology for Biofuels* 14(1), article 101. DOI: 10.1186/s13068-021-

01950-w

Kothandaraman, J., Lopez, J. S., Jiang, Y., Walter, E. D., Burton, S. D., Dagle, R. A., and Heldebrant, D. J. (2022). "Integrated capture and conversion of CO_2 to methanol in a post-combustion capture solvent: Heterogeneous catalysts for selective C-N bond cleavage," *Advanced Energy Materials* 12(46), article 2202369. DOI: 10.1002/aenm.202202369

Koutinas, A. A., Chatzifragkou, A., Kopsahelis, N., Papanikolaou, S., and Kookos, I. K. (2014). "Design and techno-economic evaluation of microbial oil production as a renewable resource for biodiesel and oleochemical production," *Fuel* 116, 566-577. DOI: 10.1016/j.fuel.2013.08.045

Liew, F. E., Nogle, R., Abdalla, T., Rasor, B. J., Canter, C., Jensen, R. O., Wang, L., Strutz, J., Chirania, P., De Tissera, S., Mueller, A. P., Ruan, Z., Gao, A., Tran, L., Engle, N. L., Bromley, J. C., Daniell, J., Conrado, R., Tschaplinski, T. J., Giannone, R. J., and Köpke, M. (2022). "Carbon-negative production of acetone and isopropanol by gas fermentation at industrial pilot scale," *Nature Biotechnology* 40(3), 335-344. DOI: 10.1038/s41587-021-01195-w

Lin, H. H., Mendez-Perez, D., Park, J., Wang, X., Cheng, Y., Huo, J., Mukhopadhyay, A., Lee, T. S., and Shanks, B. H. (2022). "Precursor prioritization for p-cymene production through synergistic integration of biology and chemistry," *Biotechnology for Biofuels and Bioproducts* 15(1), article 126. DOI: 10.1186/s13068-022-02226-7

Li, Y., Zhao, Z. (Kent), and Bai, F. (2007). "High-density cultivation of oleaginous yeast *Rhodosporidium toruloides* Y4 in fed-batch culture," *Enzyme and Microbial Technology* 41(3), 312-317. DOI: 10.1016/j.enzmictec.2007.02.008

Li, X., Gadar-Lopez, A. E., Chen, L., Jayachandran, S., Cruz-Morales, P., and Keasling, J. D. (2023). "Mining natural products for advanced biofuels and sustainable bioproducts," *Current Opinion in Biotechnology* 84, article 103003. DOI: 10.1016/j.copbio.2023.103003

Liu, C.L., Tian, T., Alonso-Gutierrez, J., Garabedian, B., Wang, S., Baidoo, E. E. K., Benites, V., Chen, Y., Petzold, C. J., Adams, P. D., Keasling, J. D., Tan, T., and Lee, T. S. (2018). "Renewable production of high density jet fuel precursor sesquiterpenes from *Escherichia coli*," *Biotechnology for Biofuels* 11, and 285. DOI: 10.1186/s13068-018-1272-z

Liu, S., Zhang, M., Ren, Y., Jin, G., Tao, Y., Lyu, L., Zhao, Z. K., and Yang, X. (2021). "Engineering *Rhodosporidium toruloides* for limonene production," *Biotechnology for Biofuels* 14(1), 243. DOI: 10.1186/s13068-021-02094-7

Magurudeniya, H. D., Baral, N. R., Rodriguez, A., Scown, C. D., Dahlberg, J., Putnam, D., George, A., Simmons, B. A., and Gladden, J. M. (2021). "Use of ensiled biomass sorghum increases ionic liquid pretreatment efficiency and reduces biofuel production cost and carbon footprint," *Green Chemistry* 23(8), 3127-3140. DOI: 10.1039/D0GC03260C

Mendez-Perez, D., Alonso-Gutierrez, J., Hu, Q., Molinas, M., Baidoo, E. E. K., Wang, G., Chan, L. J. G., Adams, P. D., Petzold, C. J., Keasling, J. D., and Lee, T. S. (2017). "Production of jet fuel precursor monoterpenoids from engineered *Escherichia coli*," *Biotechnology and Bioengineering* 114(8), 1703-1712. DOI: 10.1002/bit.26296

Neupane, B., Konda, N. V. S. N. M., Singh, S., Simmons, B. A., and Scown, C. D. (2017). "Life-cycle greenhouse gas and water intensity of cellulosic biofuel production using cholinium lysinate ionic liquid pretreatment," *ACS Sustainable Chemistry & Engineering* 5(11), 10176-10185. DOI:

10.1021/acssuschemeng.7b02116

Nora, L. C., Wehrs, M., Kim, J., Cheng, J. F., Tarver, A., Simmons, B. A., Magnuson, J., Harmon-Smith, M., Silva-Rocha, R., Gladden, J. M., Mukhopadhyay, A., Skerker, J. M., and Kirby, J. (2019). "A toolset of constitutive promoters for metabolic engineering of *Rhodosporidium toruloides*," *Microbial Cell Factories* 18, Article no. 117. DOI: 10.1186/s12934-019-1167-0

NREL. (2012). "U.S. Life Cycle Inventory Database," (https://www.nrel.gov/lci/), Accessed 10 March 2020.

Orth, J. D., Thiele, I., and Palsson, B. Ø. (2010). "What is flux balance analysis?," *Nature Biotechnology* 28(3), 245-248. DOI: 10.1038/nbt.1614

Otoupal, P. B., Ito, M., Arkin, A. P., Magnuson, J. K., Gladden, J. M., and Skerker, J. M. (2019). "Multiplexed CRISPR-Cas9-based genome editing of *Rhodosporidium toruloides*," *Msphere* 4(2), e00099-19. DOI: 10.1128/mSphere.00099-19

Peralta-Yahya, P. P., Zhang, F., Del Cardayre, S. B., and Keasling, J. D. (2012). "Microbial engineering for the production of advanced biofuels," *Nature* 488(7411), 320-328. DOI: 10.1038/nature11478

Perez-Pimienta, J. A., Papa, G., Rodriguez, A., Barcelos, C., Liang, L., Stavila, V., Sanchez, A., Gladden, J., and Simmons, B. (2019). "Pilot-scale hydrothermal pretreatment and optimized saccharification enables bisabolene production from multiple feedstocks," *Green Chemistry* 21, 3152-3164. DOI: 10.1039/C9GC00323A

Ramezan, M., Skone, T. J., Nsakala, N. Y., Liljedahl, G. N., Gearhart, L. E., Hestermann, R., and Rederstorff, B. (2007). *Carbon Dioxide Capture from Existing Coal-fired Power Plants*, National Energy Technology Laboratory, DOE/NETL Report, 401, 110907.

Rodriguez, A., Ersig, N., Geiselman, G. M., Seibel, K., Simmons, B. A., Magnuson, J. K., Eudes, A., and Gladden, J. M. (2019). "Conversion of depolymerized sugars and aromatics from engineered feedstocks by two oleaginous red yeasts," *Bioresource Technology* 286, article 121365. DOI: 10.1016/j.biortech.2019.121365

Rolf, J., Julsing, M. K., Rosenthal, K., and Lütz, S. (2020). "A gram-scale limonene production process with engineered *Escherichia coli*," *Molecules (Basel, Switzerland)* 25(8). DOI: 10.3390/molecules25081881

Rosenkoetter, K. E., Kennedy, C. R., Chirik, P. J., and Harvey, B. G. (2019). "[4 + 4]-cycloaddition of isoprene for the production of high-performance bio-based jet fuel," *Green Chemistry* 21(20), 5616-5623. DOI: 10.1039/C9GC02404B

Staples, O., Leal, J. H., Cherry, P. A., McEnally, C. S., Pfefferle, L. D., Semelsberger, T. A., Sutton, A. D., and Moore, C. M. (2019). "Camphorane as a renewable diesel blendstock produced by cyclodimerization of myrcene," *Energy & Fuels* 33(10), 9949-9955. DOI: 10.1021/acs.energyfuels.9b02557

Sundstrom, E., Yaegashi, J., Yan, J., Masson, F., Papa, G., Rodriguez, A., Mirsiaghi, M., Liang, L., He, Q., Tanjore, D., Pray, T. R., Singh, S., Simmons, B., Sun, N., Magnuson, J., and Gladden, J. (2018). "Demonstrating a separation-free process coupling ionic liquid pretreatment, saccharification, and fermentation with *Rhodosporidium toruloides* to produce advanced biofuels," *Green Chemistry* 20(12), 2870-2879. DOI: 10.1039/C8GC00518D

Sun, J., Shi, J., Murthy Konda, N. V. S. N., Campos, D., Liu, D., Nemser, S., Shamshina, J., Dutta, T., Berton, P., Gurau, G., Rogers, R. D., Simmons, B. A., and Singh, S. (2017). "Efficient dehydration and recovery of ionic liquid after lignocellulosic processing using pervaporation," *Biotechnology for Biofuels* 10, article 154. DOI:

10.1186/s13068-017-0842-9

Tan, E. C. D., Talmadge, M., Dutta, A., Hensley, J., Schaidle, J., Biddy, M., Humbird, D., Snowden-Swan, L. J., Ross, J., Sexton, D., Yap, R., and Lukas, J. (2015). *Process Design and Economics for the Conversion of Lignocellulosic Biomass to Hydrocarbons via Indirect Liquefaction. Thermochemical Research Pathway to High-Octane Gasoline Blendstock Through Methanol/Dimethyl Ether Intermediates*, National Renewable Energy Laboratory (NREL), Golden, CO (United States). DOI: 10.2172/1215006

Walls, L. E., Otoupal, P., Ledesma-Amaro, R., Velasquez-Orta, S. B., Gladden, J. M., and Rios-Solis, L. (2023). "Bioconversion of cellulose into bisabolene using *Ruminococcus flavefaciens* and *Rhodosporidium toruloides*," *Bioresource Technology* 368, article 128216. DOI: 10.1016/j.biortech.2022.128216

Wang, L., Yang, Y., Shen, W., Kong, X., Li, P., Yu, J., and Rodrigues, A. E. (2013). "CO_2 capture from flue gas in an existing coal-fired power plant by two successive pilot-scale VPSA units," *Industrial & Engineering Chemistry Research* 52(23), 7947-7955. DOI: 10.1021/ie4009716

Wang, J., Jiang, T., Milligan, S., Zhang, J., Li, C., and Yan, Y. (2022a). "Improving isoprenol production *via* systematic CRISPRi screening in engineered *Escherichia coli*," *Green Chemistry*. DOI: 10.1039/D2GC02255A

Wang, X., Baidoo, E. E. K., Kakumanu, R., Xie, S., Mukhopadhyay, A., and Lee, T. S. (2022b). "Engineering isoprenoids production in metabolically versatile microbial host *Pseudomonas putida*," *Biotechnology for Biofuels and Bioproducts* 15(1), 137. DOI: 10.1186/s13068-022-02235-6

Wang, N., Wang, D., Krook-Riekkola, A., and Ji, X. (2023). "MEA-based CO_2 capture: a study focuses on MEA concentrations and process parameters," *Frontiers in Energy Research* 11. DOI: 10.3389/fenrg.2023.1230743

Yaegashi, J., Kirby, J., Ito, M., Sun, J., Dutta, T., Mirsiaghi, M., Sundstrom, E. R., Rodriguez, A., Baidoo, E., Tanjore, D., Pray, T., Sale, K., Singh, S., Keasling, J. D., Simmons, B. A., Singer, S. W., Magnuson, J. K., Arkin, A. P., Skerker, J. M., and Gladden, J. M. (2017). "*Rhodosporidium toruloides*: A new platform organism for conversion of lignocellulose into terpene biofuels and bioproducts," *Biotechnology for Biofuels* 10, 241. DOI: 10.1186/s13068-017-0927-5

Yang, M., Baral, N. R., Anastasopoulou, A., Breunig, H. M., and Scown, C. D. (2020). "Cost and life-cycle greenhouse gas implications of integrating biogas upgrading and carbon capture technologies in cellulosic biorefineries," *Environmental Science & Technology* 54(20), 12810-12819. DOI: 10.1021/acs.est.0c02816

Zhu, Z., Zhang, S., Liu, H., Shen, H., Lin, X., Yang, F., Zhou, Y. J., Jin, G., Ye, M., Zou, H., and Zhao, Z. K. (2012). "A multi-omic map of the lipid-producing yeast *Rhodosporidium toruloides*," *Nature Communications* 3(1), article 1112. DOI: 10.1038/ncomms2112

Article submitted: February 5, 2024; Peer review completed: March 2, 2024; Revised version received: April 15, 2024; Accepted: April 22, 2024; Published: May 1, 2024.
DOI: 10.15376/biores.19.3.4056-4086

APPENDIX

Table A1. Summary of Titer, Rate, and Yield from Recent Studies

Biofuel Molecule	Host Microbes	Carbon Sources	Titer (g/L)	Rate (g/L/h)	Yield (wt %)	Theoretical Yield (wt %)*
Limonene[μ]	*E. coli*	Glucose	0.6-3.6	0.008-0.15	6-6.5	32.41
1,8-cineole[Ω]	*E. coli*	Glucose	0.65-4.37	0.076	11	36.69
Linalool[λ]	*E. coli*	Glucose	0.505	0.01	5	36.69
Epi-isozizaene[ρ]	*E. coli*	Glucose	0.728	0.01	7.3	32.41
Bisabolene[ξ]	*E. coli*	Glucose	1.15	0.015	11.5	32.41
Bisabolene[ϱ]	*R. toruloides*	Hydrolysate	1.3-2.2**	0.007-0.01	1.6-2.6	Varies[#]
Isoprenol[η]	*E. coli*	Glucose	8.5-12.4	0.1-0.15	14-18	40.9
α-Farnesene[ϱ]	*S. cerevisiae*	Glucose	38.8	0.32	-	32.41
Epi-isozizaene[ϱ]	*S. cerevisiae*	Glucose	4.7	0.04	-	32.41

[μ](Alonso-Gutierrez *et al.* 2015; Rolf *et al.* 2020). [Ω](Mendez-Perez *et al.* 2017; Lin *et al.* 2022).
[λ](Mendez-Perez *et al.* 2017; Ferraz *et al.* 2021). [ρ](Liu *et al.* 2018).
[ξ](Alonso-Gutierrez *et al.* 2015). [ϱ](Sundstrom *et al.* 2018; Magurudeniya *et al.* 2021).
[η](Wang *et al.* 2022a; Kim and Lee 2023; Kang *et al.* 2019). [ϱ](Huang *et al.* 2023)

* The theoretical yield is calculated based on the procedure outlined in the previous study, which does not account for biological constraints.

** A recent study (Walls *et al.* 2023) reported the highest reported bisabolene titer of 7.8 g/L at 144 h in *R. toruloides* utilizing organic acids.

[#] The theoretical yields of bisabolene are estimated at 32.41 wt% from glucose and xylose and at 56.3 wt% from lignin monomer (p-coumaric acid).

Table A2. Additional Data Inputs Used to Develop Process Model

Parameters	Unit	Baseline Value	Range & Standard Deviation	Probability Distribution
Biomass Composition (Baral *et al.* 2019)				
Acetate	wt%	0.9	(0.9, 2.2)	None
Ash	wt%	2.2	(2.2, 4)	None
Proteins	wt%	5.2	(4.4, 6.2)	None
Biomass Deconstruction (Magurudeniya *et al.* 2021; Sundstrom *et al.* 2018)				
IL Cost	$/kg	1	(0.5, 2)	Triangular
Pretreatment Time	h	1	(1, 3)	Uniform
Pretreatment Temperature	°C	140	(140, 140)	None
Sulfuric Acid Loading	kg/kg-IL	0.1	(0.07, 0.15)	Uniform
Sulfuric Acid Cost	$/kg	0.14	(0.14, 0.14)	None
Hydrolysis Time	h	48	(48, 72)	Uniform
Enzyme Cost	$/kg	5	(3.5, 5)	Triangular
Bioconversion (Humbird *et al.* 2011; Davis *et al.* 2018; Baral *et al.* 2023)				
Corn Steep Liquor	wt%	0.2	(0.16, 0.25)	Uniform
Diammonium Phosphate	g/L	0.3	(0.24, 0.33)	Uniform
Corn Steep Liquor Cost	$/kg	0.07	(0.05, 0.08)	None
Diammonium Phosphate Cost	$/kg	0.36	*	None
Ammonia Cost	$/kg	0.42	*	None
Compressor Pressure	kPa	310.3	*	None
Ammonia	g/L	1	*	None
Air Supply	m^3/sec	9.8	*	None
Recovery & Separation (Baral *et al.* 2019; Jones *et al.* 2014)				
Methanol Recovery	wt%	98	(95, 99)	Uniform
Hydrocarbon Fuel Recovery	wt%	98	(95, 99)	Uniform
Wastewater Treatment (Humbird *et al.* 2011; Baral *et al.* 2023)				
Nutrient Cost	$/kg	0.45	(0.3, 0.7)	Triangular
Onsite Energy & Utility (Humbird *et al.* 2011; Baral *et al.* 2023)				
Boiler Chemicals Cost	$/kg	5	(4, 6)	Triangular
Clean-In-Place Cost	$/kg	0.35	(0.35, 0.52)	Triangular
Cell Mass To Hydrocarbon (Koutinas *et al.* 2014; Jones *et al.* 2014)				
Hexane Cost	$/kg	1.19	(0.8, 1.6)	Triangular
Hydrogen Loading	mg/g-oil	2.94	*	None
Hydrotreating Temperature	°C	350	*	None
Hydrotreating Pressure	atm	35	*	None
Hydrogenation Catalyst Loading	wt%	0.012	*	None
Hydrogenation Catalyst Cost	$/kg	250	(200, 300)	Triangular
Hydrogen Loss	%	9	(9, 15)	Triangular
Phosphoric Acid Dosing	wt%	0.19	*	None
Silica Dosing	wt%	0.1	*	None
Clay Dosing	wt%	0.1	*	None
Phosphoric Acid Cost	$/kg	0.8	*	None
Silica Cost	$/kg	2.2	*	None
Clay Cost	$/kg	0.66	*	None
CO_2-To-Methanol (Ramezan *et al.* 2007; Yang *et al.* 2020; Tan *et al.* 2015)				
Monoethanolamine Cost	$/kg	1.9	(1.5, 2.3)	Triangular
GHSV of ZnO	/h	4280	*	None
GHSV of Methanol Synthesis Catalyst	/h	8000	*	None
ZnO Catalyst Cost	$/kg	10.3	(8, 15)	Triangular
Methanol Synthesis Catalyst Cost	$/kg	21.4	(18, 30)	Triangular
*The minimum and maximum values remain the same as the baseline value. GHSV = Gas hourly space velocity.				

Table A3. Greenhouse Gas Emissions Impact Vectors Combining Both Direct and Indirect Emissions

Item	Unit	Impact vector
Ionic Liquid	$kgCO_{2e}/kg$	4.75
Sulfuric Acid	$kgCO_{2e}/kg$	0.045
Enzymes	$kgCO_{2e}/kg$	7.57
Ammonia	$kgCO_{2e}/kg$	2.38
Corn Steep Liquor	$kgCO_{2e}/kg$	0.83
Diammonium Phosphate	$kgCO_{2e}/kg$	1.15
Clay	$kgCO_{2e}/kg$	0.00377
Hexane	$kgCO_{2e}/kg$	3.76
Hydrogenation Catalyst	$kgCO_{2e}/kg$	8.303
Phosphoric Acid	$kgCO_{2e}/kg$	0.56
Silica	$kgCO_{2e}/kg$	0.0212
CuO-Catalyst	$kgCO_{2e}/kg$	3.375
Monoethanolamine	$kgCO_{2e}/kg$	2.077
Methanol Synthesis Catalyst	$kgCO_{2e}/kg$	5.905
Renewable Hydrogen	gCO_{2e}/kg	6.08
Diesel	gCO_{2e}/kg	4.12
Fossil Methanol	$kgCO_{2e}/kg$	1.73
Electricity (U.S. Mix)	$kgCO_{2e}/kWh$	0.43

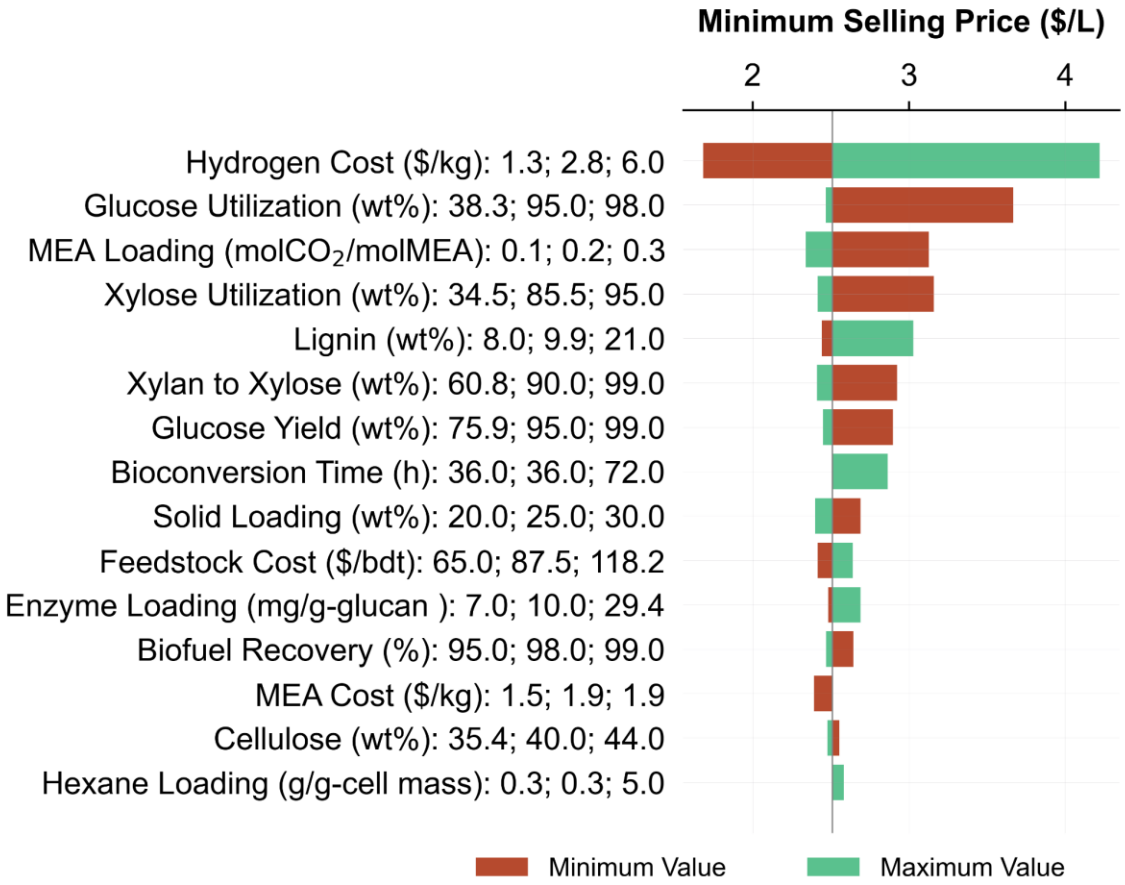

Fig. A1. Most influential inputs to the minimum selling price of bisabolene in a representative case considering both cell mass and CO_2 utilizations. The first, second, and third values of each input parameter represent the minimum, baseline, and maximum values, respectively. MEA = Monoethanolamine. bdt = bone-dry metric ton.

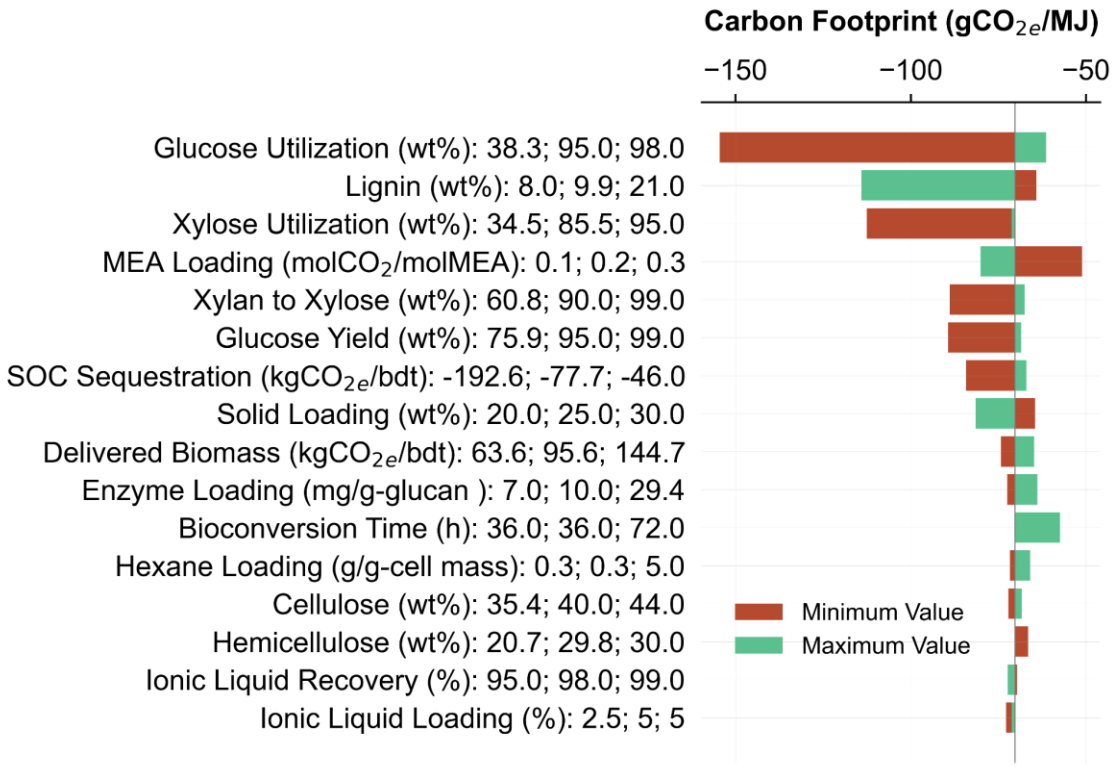

Fig. A2. Most influential inputs to the greenhouse gas emissions of bisabolene in a representative case considering both cell mass and CO_2 utilizations. The first, second, and third values of each input parameter represent the minimum, baseline, and maximum values, respectively. MEA = Monoethanolamine. SOC = Soil organic carbon. bdt = bone-dry metric ton.

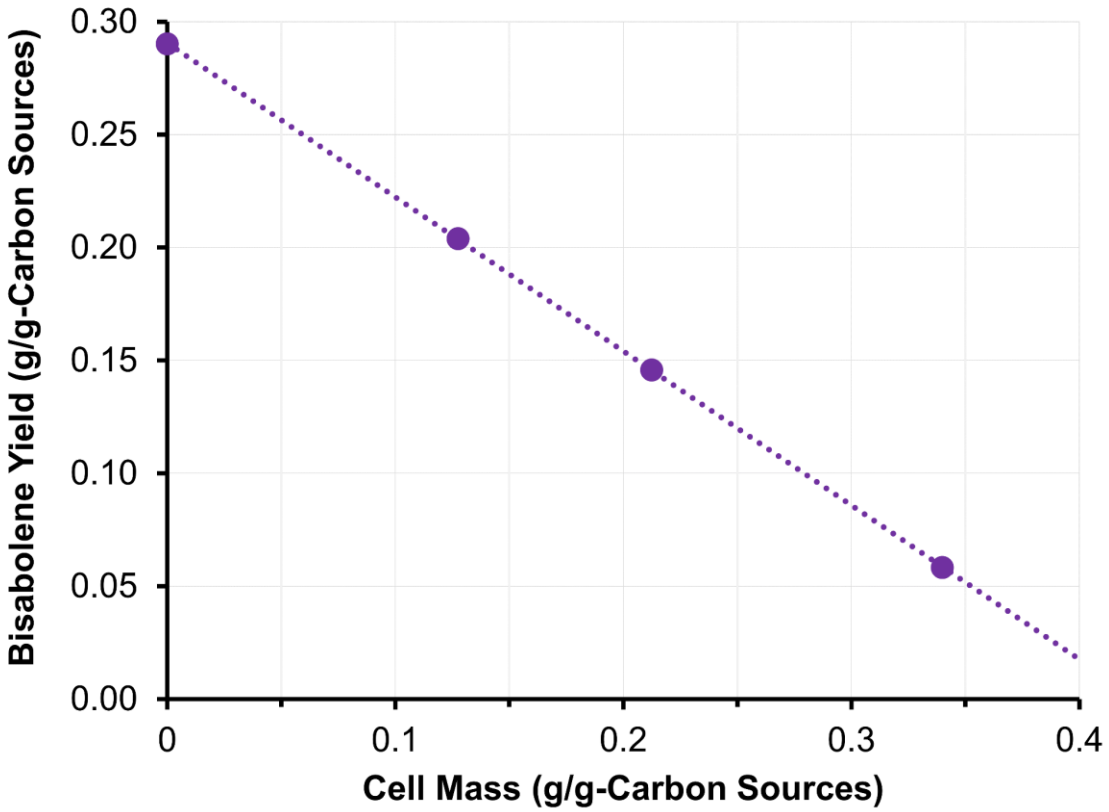

Fig. A3. Relationship between bisabolene and cell mass yields. The results are obtained from the genome-scale metabolic model analysis performed in this study. The recent genome-scale metabolic model for *R. toruloides,* Rt_IFO0880 (Kim *et al.* 2020) and flux balance analysis (FBA) (Orth *et al.* 2010) was used to calculate the maximum theoretical yields for cell mass and bisabolene from reaction stoichiometry and redox balance. COBRA Toolbox v.3.0 (Heirendt *et al.* 2019) in MATLAB R2017b was used for FBA simulations with the GLPK (https://gnu.org/software/glpk) or Gurobi Optimizer 8.1 (http://www.gurobi.com/) as the linear optimization solver.